5-2023

Visual Working Memory Encoding and Action: An Investigation using fNIRS and Mouse-tracking

Kaleb Thomas Kinder
kkinder5@vols.utk.edu

To the Graduate Council:

I am submitting herewith a dissertation written by Kaleb Thomas Kinder entitled "Visual Working Memory Encoding and Action: An Investigation using fNIRS and Mouse-tracking." I have examined the final electronic copy of this dissertation for form and content and recommend that it be accepted in partial fulfillment of the requirements for the degree of Doctor of Philosophy, with a major in Psychology.

Aaron T. Buss, Major Professor

We have read this dissertation and recommend its acceptance:

A. Caglar Tas, Daniela M. Corbetta, Jared M. Porter

Accepted for the Council:

Dixie L. Thompson

Vice Provost and Dean of the Graduate School

(Original signatures are on file with official student records.)

Visual Working Memory Encoding and Action: An Investigation using fNIRS and Mouse-tracking

A Dissertation Presented for the
Doctor of Philosophy
Degree
The University of Tennessee, Knoxville

Kaleb Thomas Kinder
May 2023

ACKNOWLEDGEMENTS

Firstly, I would like to thank my advisor, Aaron Buss, for his guidance and effort in training me. I am grateful for the intellectual freedom you provided me to pursue my research interests while always posing the right questions to steer my projects towards more interesting conclusions. You put in a great deal of your time into reviewing my projects, editing my writing, and teaching me new skills; I am a much better independent researcher because of it. I am also grateful to Caglar Tas for her advising throughout my time in graduate school. Thank you so much for including me in your lab and guiding me like you would your own PhD student. I have benefited so much from our discussions and project collaborations. Thanks as well to my committee members, Daniela Corbetta and Jared Porter, for all their feedback and valued input on my dissertation project.

During my time at the University of Tennessee, I have benefited greatly from the support of everyone in the Buss and Tas labs. A special thanks to Jessica Defenderfer for sharing her time and helping me with all things fNIRS related while making it so much fun. I would also like to thank our fantastic lab manager, Rachel Eddings, for her help with all the finer details involved in setting up my dissertation project and guiding me through the fNIRS data processing pipeline. Thanks also to my lab mates over the years in the Buss (Anastasia Kerr-German, Kara Lowery, Hollee Heim, Alexis McCraw, & Jackie Sullivan) and Tas lab (Jessica Parker, Michael Mugno, Madeline Embrey, & Golnaz Forouzandehfar) for their friendship and support. I would also like to acknowledge all the help and hard work from the undergraduate research assistants in both labs (Ali Bhimani, Morgan Sizemore, James Cooper, & Ellie Pritchard) who made this dissertation project possible.

To my close friend, Tim Coffey. This moment has me reflecting on the countless hours we spent simply being together talking, usually late-night on a porch, and soul-searching while growing up. Our time together was (and still is) so important to my learning how to think and consider different perspectives. You showed me that even a kid from a small, rural town like Goreville can challenge the status quo and chart the path less taken. Thank you for your insights, your inspiration, and most importantly for your friendship; you are a fundamental part of my academic and personal journey.

To my parents, a special thank you for all your love and for encouraging me to follow my dreams. Dad, you have had to overcome so many obstacles in life and I often look to that for inspiration. You worked so hard to get where you are, and I can only hope a portion of that work ethic and drive has rubbed off on me. Thank you as well for being my biggest fan no matter the activity I took up, whether it be sports, a hobby, or an academic endeavor. Mom, thank you for all the personal sacrifices you made to even make this moment possible for me. You dedicated so many hours and always put me and my brother first before anything else. I would not be here without everything you've done. I would also like to extend my thanks to my stepparent, Kari. Thank you for showing a genuine interest in my research and for being a continuous source of support through this process. To my brother, Kyle. Thank you for all the years of support, and for distracting me when I needed it most: What a save! You are an incredible little brother and friend. I couldn't imagine having taken this path without you. Last and certainly not least, I want to thank my partner Abby for your constant encouragement and support throughout all of this. Thank you for being there every day, listening to my successes and setbacks, brainstorming research ideas, contributing to my well-being during graduate school, and for always believing in me. You made this research a lot more fun to carry out.

Dedicated to future first generation college students.

ABSTRACT

Visual working memory (VWM) guides the motor system by temporarily keeping relevant information in mind. As an interface between perception and action, VWM plays a critical role in supporting goal-directed behavior. Research on the relationship between VWM and action has primarily focused on the effect of VWM on motor output. Traditional approaches index outcome responses, such as accuracy, but this practice provides limited information on underlying VWM processes. Conversely, the influence of action on VWM processes has received less attention and its neural correlates are not well understood. In this thesis, I examined VWM-action links using functional near-infrared spectroscopy (fNIRS) and mouse-tracking to record real-time trajectories of participants' motor responses. Experiment 1 aimed to understand the relationship between movement dynamics, VWM performance, and their associated neural activity in a standard change detection task. Experiments 2 and 3 focused on the effect of action on VWM encoding using change detection tasks that manipulated task-relevance of the action (Experiment 2) and action-relevance of the items held in VWM (Experiments 2 & 3). The results showed that action enhanced VWM encoding for action-relevant features but impaired memory for action-irrelevant features. Moreover, the frontoparietal VWM network was differentially associated with action-relevant and action-irrelevant memory performance. Together, these findings suggest a trade-off between action and VWM encoding, where the representations of action-relevant features are prioritized but action-irrelevant features are suppressed. These results support and expand on the motor-induced encoding effect, demonstrating how action enhances VWM encoding for features that are action-relevant.

TABLE OF CONTENTS

LIST OF TABLES

LIST OF FIGURES

Chapter 1: Introduction

Goal-directed behavior is demonstrated by the ability to orient and interact accordingly with the surrounding environment. Integral to this ability is the interface between perception and action: utilizing relevant environmental input to create a motor response that produces a desired outcome. This process involves engaging the motor system to stimuli in the environment that satisfy internal goals or task demands. *Visual working memory* (VWM; Baddeley, 1992, 2003) is a cognitive function that plays a critical role in this process by holding goal-relevant information in mind, enabling flexible interaction with the environment. Even the simplest of everyday activities requires accessing the privileged information temporarily held in VWM. However, only a very limited amount of information can be held in VWM at any given time, with average capacity limits typically around 3-4 simple pieces of information (e.g., remembering different colors; Cowan, 2001). Despite this low number, there is considerable individual variability in capacity estimates, which are highly predictive of several positive cognitive constructs such as cognitive control (Unsworth et al., 2012; Gulbinaite, 2014; Cowan et al., 2005), problem-solving (Alloway et al., 2009; Tillman et al., 2008) and fluid intelligence (Fakuda et al., 2010; Unsworth et al., 2015). Therefore, a fundamental research goal in the cognitive sciences is to better understand the behavioral and neural interactions that underlie VWM, its relation to other cognitive processes, and ultimately how it supports goal-directed behavior.

A standard approach to assessing VWM is using the change detection task (Luck & Vogel, 1997). In the canonical change detection task, an array of items is briefly presented to be encoded into VWM, followed by a short maintenance interval, and then a test array that either contains the same items that were previously shown or one of the items changes (e.g., a color change). Researchers have used the change detection task to extensively probe VWM processes.

For example, this task can reliably differentiate between individuals with high and low VWM capacity (Dai et al., 2019). Moreover, individual VWM performance measured with the change detection task has been shown to remain highly stable over time and across multiple measurements (Xu et al., 2018). This makes the change detection task well-suited for investigating the relationship between VWM and action.

Several studies have examined VWM and how it can be enhanced. Luria et al. (2016) suggested that attentional control may contribute to individual differences in VWM capacity. According to this perspective, attentional control limits distractor information from entering VWM. In other words, individuals with superior attentional control may have more top-down resources available for representing goal-relevant information in VWM (also see Melcher & Piazza, 2011). Attentional control training has been shown to significantly enhance VWM performance in individuals with low VWM capacity (Li et al., 2017), providing support for the importance of attentional processes in VWM performance. These results provide evidence that individual differences in attentional processes are important contributors to VWM performance. Another construct that works closely with attention processes is action, yet the role of action in VWM performance is less studied. In the following sections, I review evidence for bidirectional VWM-action links and point to open questions in this line of work. The first goal of this thesis is to investigate the relationship between motor dynamics and VWM performance. The second goal will be to determine whether action during VWM encoding modulates VWM performance.

Action and cognition: Bidirectional links

Traditionally, the motor system was viewed as an output of cognition and treated as distinct from perceptual and cognitive processes. Under this framework, information flowed in cognition in a single direction across different stages. These stages typically involve (1)

perceptual processing of a stimulus, (2) converting perceptual information to a symbolic code that permits the abstract representation of the stimulus, (3) decision-making processes to determine the appropriate behavioral response, and (4) motor output to execute the chosen response (Sternberg 1969). However, an abundance of research has since shown that the motor system influences cognition and that the two systems interact with each other in ways that go beyond a simple input and output relationship.

There is extensive research from various fields that supports the idea of bidirectional links between action and cognition. One such field is vision sciences, where studies have found a connection between visual attention and action preparation and execution. These studies have demonstrated that a saccade or reaching behavior to a spatial location improves visual attention to that location (Hoffman & Subramaniam, 1995; Baldauf et al., 2006), and enhances the discrimination of targets prepared movement location (Schneider & Deubel, 1995). Moreover, features of stimuli that are action-relevant have been shown to receive heightened perceptual processing (Bosco et al., 2017). In the following sections, I review the current body of literature on the bidirectional relationship between VWM and action (as depicted in Figure 1). The review begins by discussing research demonstrating how VWM guides action and how the contents of VWM can impact motor behavior. Next, I discuss research on the impact of action on VWM and long-term memory. Finally, I discuss neuroimaging studies on the VWM network and propose potential neural networks involved in the effect of action on VWM encoding.

VWM guides the motor system

VWM and the motor system closely coordinate to generate purposeful behavior. VWM actively preserves previously seen visual information for future interaction with the environment, making it a mediator between perception and action processes. Guiding future actions is a central

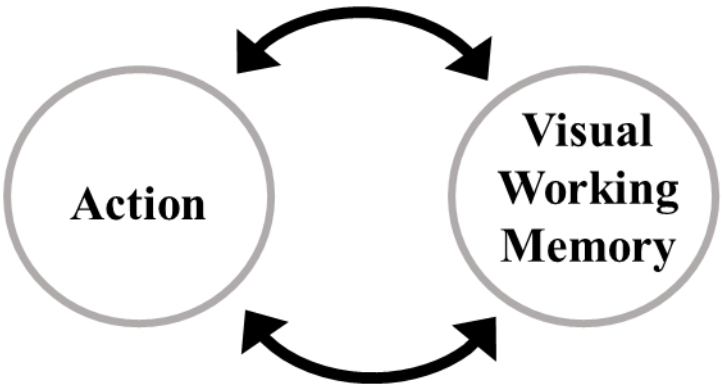

Figure 1. Bidirectional Links between Action and Visual Working Memory

concern of VWM (Allport, 1987; Ballard et al., 1997; Prinz et al., 2013), as it stores information that is no longer visible to guide the motor system toward potentially relevant stimuli. VWM is particularly important for guiding precise motor movements. For example, the size and shape of an item stored in VWM can determine whether a large gripping action or a fine gripping response is necessary (e.g., Grèzes et al., 2003). Below, I discuss research exploring the automatic recruitment of VWM processes during action and how VWM can affect the motor system.

VWM is recruited by action

One type of action where VWM may be fundamental is eye movements. Eye movements occur rapidly, constantly scanning the environment for relevant visual input. To do this, eye movements rely on past visual information to update retinal inputs across saccades to view the external environment continuously (i.e., transsaccadic updating). The maintenance of information across a saccade has been proposed to rely on VWM processes (e.g., Aagten-Murphy & Bays, 2019; Tas et al., 2016). That is, eye movements may recruit VWM processes to perceive the world in a stable state. VWM processes have also been implicated in guiding other forms of movements too, such as reaching behavior. It is well established that action preparation enhances the visual perception of action-relevant features of an item, such as its size and orientation (e.g., Bosco et al., 2017; Gutteling et al., 2011). In line with these findings, neuroimaging research has evaluated whether early visual cortex is recruited by motor preparation and execution to explain enhanced visual perception of action-relevant features. Gutteling et al. (2015) showed with fMRI that different movement behaviors (e.g., grasp or pointing) could be decoded with high accuracy from signals in early visual cortex. Furthermore, signals in V1 could predict the type of response for both movement execution and movement

preparation. These results have also been found in situations where visual input is not present (i.e., complete darkness) at the time of the action (Monaco et al., 2018; Singhal et al., 2013), further suggesting that the contents in VWM may be recruiting early visual areas during movement preparation.

VWM influences action

Information held in VWM has also been shown to influence prospective actions. A common method for examining this relationship is using a visual search task and manipulating the contents of VWM. One way this is studied is by using a dual-task paradigm where a visual search task is performed during the maintenance interval of a VWM task. Visual search has been shown to be biased if one of the items (a distractor or the target) in the search array matches an item held in VWM (e.g., the shape of item held in VWM; Han & Kim, 2009; Hollingsworth & Luck, 2009; Olivers, 2009; Olivers et al., 2006; Soto et al., 2006), an effect termed memory-driven capture. Items held in VWM in an active state, as opposed to an accessory or passive state, are particularly prone to bias attention and responses in visual search tasks (Olivers et al., 2011).

The contents of VWM have also been shown to impact eye movement trajectories. For example, Theeuwes et al. (2005) asked participants to remember the spatial location of a dot in a memory condition. Participants then performed an eye movement to a target located either to the left or right where the memory item had been. Compared to a no-memory condition, it was found that saccades curved away from the spatial location of the memory item. The authors proposed that deviation from the memory item reflected a strong overlap of the VWM and eye movement systems, such that the memory item was inhibited during the eye movement (also see Boon et al., 2014; Belopolsky & Theeuwes, 2011). Further, eye movements have been shown to curve away

from the location if the item was still visually present (e.g., Doyle & Walker, 2001). Together, these results demonstrate that visual perception and the contents of VWM can modulate motor dynamics.

The motor system influences VWM

It has also been demonstrated that the motor system influences VWM processes, consistent with the action-oriented approach to studying cognition (Thelen & Smith, 1994; Chiel & Beer, 1997). Research in this area has primarily focused on how actions during the maintenance interval can modulate the contents of VWM. One common approach to examining actions' influence on VWM is with a dual-task that cues participants to execute a hand movement to a spatial location during the maintenance interval of a memory task. The item location of the movement may then be cued during the memory test phase (action-relevant), or another non-movement location may be cued (action-irrelevant). The typical finding is that items presented in action-relevant locations result in better memory than items at action-irrelevant locations (Heuer et al., 2017; Ohl & Rolfs, 2018, 2020; Hanning et al., 2016). This effect, termed selection-for-action, has been proposed to occur by an attentional prioritization of items at action-relevant locations; however, it remains unclear whether selection-for-action enhances action-relevant items, inhibits action-irrelevant items, or if the effect is a combination of both (Heuer et al., 2020). While there are still open questions in this line of research, these results provide strong evidence that motor processes can modulate the contents of VWM.

Similarly, Tas et al. (2016) showed that the overt execution of a saccade to an object during the retention interval automatically encodes the object into VWM. In a series of experiments, participants performed change-detection tasks. During the retention interval, participants either overtly shifted attention via a saccade to a secondary, irrelevant object or

covertly shifted attention to the presence of the object while maintaining central fixation. Performance on the change-detection task was impaired when saccade execution was required during the maintenance interval compared to when no saccade was required. These results suggest that saccade execution automatically led to VWM encoding of the secondary object, thus increasing VWM load and impairing memory for the objects relevant to the change-detection task. Importantly, these results suggest that actions may automatically recruit VWM processes and impact the representation of items held in VWM.

Recent research has also shown an effect of motor processes on long-term memory encoding. Yebra et al. (2019) was the first to show that executing simple motor responses (e.g., a button-press) enhances long-term memory encoding, an effect they termed action-induced memory enhancement. In a series of go/no-go tasks, participants were instructed to execute responses to one type of stimulus (go trials) and inhibit responses to another stimulus type (no-go trials). Across their experiments, the authors found better memory for go trials than no-go trials. Functional magnetic resonance imaging (fMRI) results showed engagement of the locus coeruleus on go trials, known to release noradrenaline, an important neural resource for improving memory encoding (Strange & Dolan, 2004). Based on these results, the authors concluded that executing a motor response led to enhanced memory encoding. In addition to action execution, the degree of motor engagement, including motor preparation, has been shown to enhance long-term memory encoding (Kinder & Buss, 2021). Using a modified go/no-go task, we found that go stimuli had better memory than no-go stimuli (replicating the results of Yebra et a., 2019). Importantly, however, when compared to a motor-neural condition we found that both go (motor execution), and no-go trials (motor preparation) had better memory scores. We interpreted these results to reflect a graded effect of motor engagement on memory encoding, an

effect we termed *motor-induced encoding*. Together, these studies provide evidence that motor processes can affect cognitive processes such as attention and long-term memory.

As reviewed here, several lines of work have examined the bidirectional link between action and memory. However, one aspect that has not been examined is whether action modulates VWM encoding. Although research has shown that action modulates the contents of VWM during the maintenance interval (Heuer et al., 2017; Heuer et al., 2020), it is still unclear whether action modulates VWM representations as they are being encoded. This open question builds upon our previous work (Kinder & Buss, 2021), which revealed that motor engagement enhances memory encoding for items in long-term memory. In this thesis, I investigate whether the motor-induced encoding effect can be extended to VWM encoding.

Motor-induced encoding in VWM: Neural mechanisms

Neuroimaging research supports a close link between memory and motor systems, as these systems significantly overlap (Jonikaitis & Moore, 2019; Ikkai & Curtis, 2011). For example, single-cell recordings of the posterior parietal cortex (PPC) in rhesus monkeys suggest activity of a population of neurons tuned to remembering a location persists during the maintenance interval and into movement preparation (Anderson & Buneo, 2002; Anderson & Cui, 2009; Quiroga et al., 2006). Specifically, these studies have provided evidence that the intraparietal sulcus (IPS) in PPC is involved in motor engagement and VWM. Additionally, it has been proposed that action can enhance long-term memory encoding via the locus coeruleus (Yebra et al., 2019), which is a part of the noradrenergic system that promotes successful memory encoding by releasing noradrenaline (Strange & Dolan, 2004).

Another possibility is that motor engagement could improve VWM encoding through an attentional network that includes top-down signals from frontoparietal regions that influence

VWM representations in early visual areas (Pasternak & Greenlee, 2005). The dorsal attention network (DAN) includes multiple frontoparietal regions involved in memory and action, including the IPS, superior parietal lobule (SPL), and pre-SMA. It is also involved in modulating the top-down deployment of attention (Vossel et al., 2014) and has been associated with stimuli eliciting high motor engagement and activation in the pre-SMA (Koldny et al., 2017). Because the pre-SMA scales in activation during motor preparation until motor execution, it is a potential candidate for sending top-down projections to visual areas that enhance VWM memory as motor engagement increases. However, other frontal regions such as the middle frontal gyrus (MFG) and superior frontal gyrus (SFG) also play a role in VWM (Riley & Constantinidis, 2016). The neural networks proposed here underlying the motor-induced encoding effect are speculative, and it is possible that motor engagement could enhance VWM encoding via a distributed network. In this thesis, the neural correlates of the motor-induced encoding effect will be explored by recording cortical activation in frontoparietal regions using functional near-infrared spectroscopy (fNIRS).

Present study

This review highlights that the VWM and motor system are closely linked and interact bidirectionally. Although research has demonstrated that action affects the contents of VWM during maintenance, it remains unclear how motor processes influence VWM during encoding. This thesis aims to address this knowledge gap by using a combination of continuous behavioral and neural measurements. In three experiments, I concurrently measured movement trajectories via mouse-tracking and cortical activation via fNIRS in change detection tasks. These experiments included a standard version of the change detection task (Experiment 1) and investigated the effects of different motor responses on VWM encoding (Experiments 2 & 3)

The traditional approach to measuring motor responses and performance in change detection tasks has relied on outcome responses, typically accuracy. Although informative for calculating the number of items successfully held in VWM (Pashler, 1988), this practice provides limited information on the behavioral dynamics underlying VWM performance.
In recent decades, accumulating evidence suggests that movements continuously interface with cognitive processes in real-time, suggesting that using a movement tracking method could provide a more direct observation of cognition. Neurophysiological research provides further support for the continuous updating of motor output during cognitive processing. For instance, Cisek and Kalaska (2005) demonstrated that activity in the premotor cortex dynamically unfolds throughout a decision. In that study, monkeys were tasked with reaching toward one of two response options. Single-cell recordings over the premotor cortex initially showed that directionally tuned neurons simultaneously activated for both response options as the reaching movement began. Importantly, as the reaching behavior unfolded, activation for the selected location gradually increased while, simultaneously, activation for the unselected response location was gradually inhibited. Furthermore, it was found that activation in the premotor cortex could reliably predict the eventual reaching response location and if there would be a reaching error. These findings suggest that a real-time movement tracking method could provide a more comprehensive understanding of the relationship between motor processes and VWM performance.

Behavioral evidence in humans also supports the dynamic activation of multiple response options. Spivey et al. (2005) demonstrated this in language recognition by asking participants to move and select one of two words, such as candy and candle, after hearing a phrase (e.g., "select the candy"). When the incorrect response (e.g., candle) overlapped with some of the phonemes

for the correct response (e.g., candy), movements tended to be initially attracted either toward the incorrect response or between the response options before gradually transitioning back toward the correct response. This demonstrated that movement trajectories continually evolve during language recognition, indicating partial activation of each response option at different points of the movement. Additionally, movement trajectories have been shown to index participants' long-term memory strength (Papesh & Goldinger, 2013). In this study, participants made old/new responses to stimuli in a memory task and then rated their confidence along a 1-7 rating scale. As measured with mouse-tracking, participants' movement trajectories predicted their confidence estimates. Specifically, more linear, and faster movement trajectories were associated with stronger memories, whereas more curvilinear and slower movement trajectories were associated with weaker memories. Therefore, in the proposed experiments, mouse-tracking will be used in a change detection task to index VWM strength.

In the first experiment, I recorded real-time movement trajectories and cortical activation in a standard change detection task. Participants moved a mouse cursor to one of two response locations that indicate either a "same" or "different" response. The task utilized four VWM set sizes, ranging from set sizes 2-5. First, I will investigate whether VWM capacity estimates replicate the findings commonly seen in button-press versions of the change detection task. I predicted that higher set sizes would be linked to more activation in PPC (Todd & Marois, 2004, 2005), and movement trajectories would be more curvilinear and slower to move toward the correct response. Further, I predicted that trials with less curvature would be associated with greater activation in the VWM frontoparietal network.

In the subsequent experiments I recorded real-time movement trajectories (Experiments 2 & 3) and cortical activation (Experiment 3) in modified change detection tasks. In alternating

blocks, participants either performed either a "no-movement" or a "move" change detection task. In the move version of the change detection task, participants were tasked to engage in a simple motor movement (i.e., button-presses) during memory encoding. The no move change detection task was identical to the move change detection task, except that there was no motor engagement during memory encoding. A set size of 4 was used to examine VWM performance near the average VWM capacity estimate (~3-4 items). First, I predicted VWM performance would improve when participants executed motor responses during memory encoding compared to no movement, consistent with the motor-induced encoding effect. I also hypothesized that activation in the frontoparietal VWM network during encoding would predict subsequent VWM performance. That is, greater activation in these regions should be associated with movement trajectories that are less curvilinear, indicating VWM performance. Finally, I hypothesized that individual motor dynamics, such as trajectories' curvature, would predict VWM outcome performance measures, such as accuracy.

Chapter 2: Experiment 1

The main objective of Experiment 1 was to examine VWM performance and its neural correlates using a mouse-tracking adaptation of the standard change detection task. Specifically, this experiment aimed to determine whether the dynamics of participants' movements (i.e., response curvature) would vary based on VWM demands (i.e., higher set sizes) and activity in VWM regions of interest. The task (illustrated in Figure 2) required participants to attend to the color of the items in a brief encoding display, followed by a test display where participants moved the mouse-cursor to select a response (upper-left or upper-right response location), indicating whether the items had changed or remained the same. The subsequent experiments followed a similar experimental structure, but with motor manipulations during the encoding display.

Methodology

Participants

Participants included 36 undergraduate students (30 female) ranging from 18-28 years of age from the University of Tennessee, Knoxville. One participant was dropped due to a color vision deficiency being detected with the Ishihara Test for Color Blindness (Clark, 1924), resulting in a final sample size of 35 participants. The final sample of participants all had normal or corrected-to-normal vision and were right-handed. The required sample size was calculated with a power analysis based on the results of a separate pilot study (N = 7) of the same design. The power analysis was run with the MorePower 6.0 program (Campbell & Thompson, 2012). For a 2 (change: same, different) x 4 (set size: SS2, SS3, SS4, SS5) within-subjects design, we calculated the required sample size to achieve a power of .9. I calculated the most conservative sample size estimate between the effects of change (η_p^2 = .765), set size (η_p^2 = .152), and change

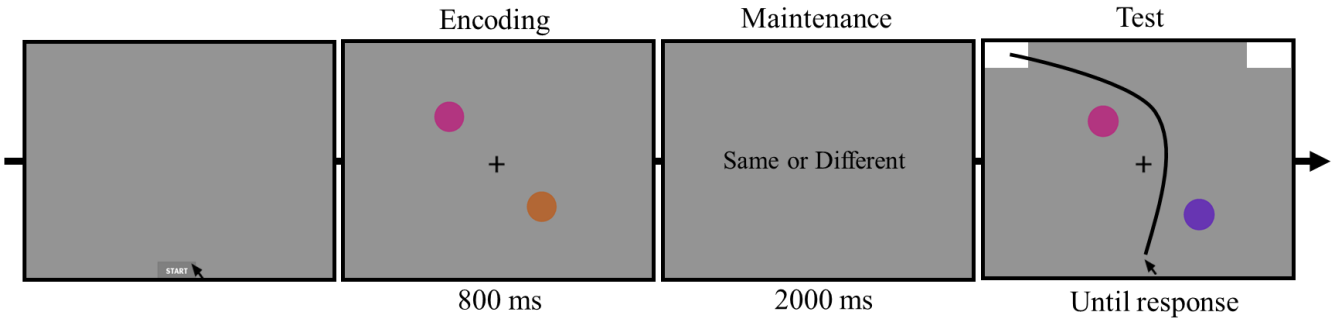

Figure 2. Experiment 1 Trial Sequence. Participants initiated each trial by clicking on the "Start" button. An encoding array of colored circles then appears, followed by a blank maintenance interval, and then a test array. The colored circles in the test array can be either the same color as those in the encoding array (same trial) or one of the colors changes (different trial). In this example, the set size is 2 and there is a color change. In this instance, the "same" response is associated with the top-right response location and the "different" response is associated with the top-left response location during the test array.

x set size interaction (η_p^2 = .286) on curvature scores. The power analysis showed that a minimum of 28 participants were needed to achieve .9 power to detect a set size curvature effect of η_p^2 = .152. I opted to oversample, aiming to recruit 36 participants in anticipation of potential exclusions. The same target sample size of 36 participants was used for all subsequent experiments. Participants provided informed consent, completed a demographics survey upon arrival, and were compensated with course credit upon completion of the study. The University of Tennessee Institutional Review Board approved the proposed study's protocols.

Apparatus and stimuli

The change detection task was displayed on a 20.5 x 11.5-inch LCD computer monitor with a resolution of 1920 x 1080 pixels and a refresh rate of 60Hz. Participants were seated approximately 60 cm from the computer monitor. Stimuli were presented via an online interface of the MouseTracker (Freeman & Ambady, 2010) and MATLAB R2022a (Natick, Massachusetts: The MathWorks Inc.) software. The x and y coordinates of participants' mouse cursor movements were recorded on the screen at a sampling rate of 60Hz. Each trial began when participants clicked a "Start" button at the center bottom of the screen, subtending ~4.9 x 1.7 degrees of visual angle (dva). Next, a fixation cross appeared at the center of the screen, subtending ~.45 x .45 dva. The response locations were white rectangles (RGB: 255, 255, 255) located at the upper-left and upper-right corners of the screen. The response locations subtended ~7.2 x 3.5 dva. Stimuli were circles that varied in HSV color space. Six colors were generated on each trial such that at least 60º separated each color in color space. Colored circles were randomly selected from this pool to be displayed on the stimulus array on a uniform gray background (RGB: 148, 148, 148). These items, each subtending ~1.7 x 1.7 dva, were randomly placed along positions of an imaginary circle (radius of ~3.23 dva), also separated by at least 60º.

Design and procedure

The basic structure of the task is illustrated in Figure 2. Each trial was initiated when participants clicked on the "Start" button. A fixation cross was then presented for 500 ms at the center of the screen. After fixation offset, the encoding display was presented for 800 ms, followed by a maintenance interval of 2000 ms, and then the test display was presented until a response was recorded. Intertrial intervals varied trial by trial based on the amount of time participants took to click the "Start" button. However, a minimum intertrial interval of 500 ms was implemented. Participants were instructed to attend to and remember the items that appeared during the encoding display. There were set sizes of either 2, 3, 4, or 5 items presented during the encoding display. During the test display, the colors of the items in the array reappeared and either stayed the same (same trial) or one of the colors changed (different trial). Same and different responses were mapped to the upper-left and upper-right response locations (equally counterbalanced across participants). The mouse cursor was locked at the Start location until the onset of the test display. Participants were instructed to initiate moving the mouse cursor as quickly as possible once the test display appeared. This standard mouse-tracking instruction promotes movement dynamics that coincide with ongoing cognitive processes (Freeman & Ambady, 2009) as opposed to movements occurring after a decision is already made. Participants had 500 ms to initiate movement once the test display appeared, or the message "Please start moving earlier even if you are not fully certain of a response yet!" was presented. Trials with this message were discarded from further analyses.

Set size (2, 3, 4, & 5) and trial type (same, different) were randomly mixed in 2 blocks of 140 trials per block, with 280 total trials (Table 1). There were an equal number of trials per condition (35 trials each). Participants received a short break between blocks. There were eight

Table 1. Summary of participants and experimental context for each experiment

Experiment	Encoding Time	Maintenance Time	Set Size	Encoding Movement	Trial #	Context	*N*
1	800ms	2000ms	2,3,4, & 5	No	280	fNIRS	35
2	800ms	2000ms	4	Yes	240	Behavioral	33
3	800ms	2000ms	4	Yes	200	fNIRS	32

practice trials, with one practice trial per condition. Participants were shown example sequences of trials to become familiarized with the task before the practice trials. Overall, the task lasted approximately 40 minutes.

Mouse-tracking methods

Data preprocessing

Movement trajectories along the *x*- and *y*-axes were rescaled into a standard coordinate space (bottom left: [-1,0]; top right: [1,1.5]). Trajectories to the left response location were remapped to the right location, resulting in the overlay of all trajectories to the same response location. Spatial (i.e., the proximity of the mouse cursor to each response location) mouse-tracking data were extracted. For spatial data preprocessing, trajectories were normalized into 101-time steps to compare trials of varying response times. After spatial normalization, the x and y coordinates at each of the 101-time steps were averaged for each participant (Freeman & Ambady, 2010).

Trials were excluded from the following analyses based on the criteria of my previous work (Kinder et al., 2022): Incorrect trials (8.82% of trials), slow RTs (two standard deviations above the mean; 3.65% of trials), slow movement initiations (two standard deviations above the mean; 2.10% of trials), and abnormal trajectories (two standard deviations above and below the mean AUC; 7.58% of trials). Overall, 11.79% of trials were excluded from the following analyses, not including the accuracy analyses.

fNIRS methods

Data acquisition and probe design

fNIRS data were collected with a 29-channel (3 cm separation; 8 sources and 16 detectors) TechEn CW7 system (TechEn Inc., Milford, Massachusetts) at a sampling rate of 25

Hz. Near-infrared wavelengths of 830nm and 690nm were used to record changes in HbO and HbR concentration during the change detection tasks in Experiments 1 and 3 (Table 2). The source-detector configuration (Figure 3) contained 29 channels separated by 30mm and 2 short channels separated by 10mm. Short source-detector channels were used to regress out extracerebral artifacts (Goodwin, 2014). Channels were distributed over the right frontal cortex, motor cortex, and posterior parietal cortex to target regions of interest related to memory, action, and attention (Table 2). Participants wore a 60cm circumference fNIRS custom cap fitted with the source-detector channels. After cap placement, a Polhemus digitizing system was used to obtain the spatial coordinates of the sources and detectors and to map their location in reference to each participant's anatomical landmarks (nasion, left and right preauricular, inion, and vertex (CZ)). Before beginning data collection, these points were mapped onto a brain atlas using the AtlasViewer toolbox (Aasted et al., 2015) and visually inspected for probe placement accuracy. fNIRS signal quality was also visually inspected with the TechEn CW7 system before data collection began to enhance signal quality.

Preprocessing for channel space

fNIRS data were pre-processed in MATLAB R2022a (Natick, Massachusetts: The MathWorks Inc.) using the Homer2 software (Huppert, 2009). The preprocessing options used in Defenderfer et al. (2022) were used in the following channel space processing steps, which are described below. fNIRS data were first converted to units of optical density. The data were then processed using a combined approach of spline interpolation and Savitzky-Golay filtering techniques (Savitzky & Golay, 1964), with a frame size of 10s and a p-value of 0.99, to correct for significant spikes and baseline shifts. To minimize motion artifacts, we employed the hmrMotionCorrectWavelet method (Molavi & Dumont, 2012) with an IQR threshold of 0.72.

Table 2. fNIRS Recorded Regions of Interest

Anatomical Region	Hemisphere	MNI Scalp Coordinates (x, y, z)	Nearest Brodmann's Area
Precentral gyrus	R	29, -22, 95	6
Superior frontal gyrus	R	26, 40, 74	8
Middle frontal gyrus	R	62, 39, 35	9
Inferior frontal gyrus	R	72, 32, 7	45
Superior parietal lobule	R	30, -52, 93	7
Angular gyrus	R	47, -78, 61	39

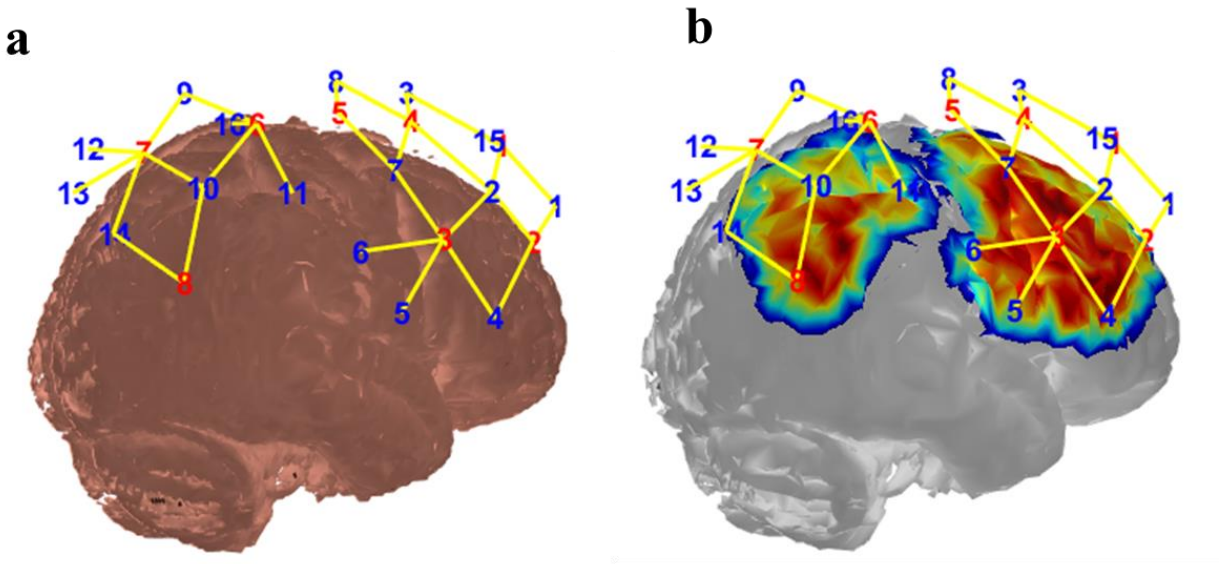

Figure 3. fNIRS probe configuration and sensitivity profile. **a.** fNIRS source and detector configuration to record from the regions of interest. Eight light detectors and 16 light sources were used to generate 29 source-detector channels. Channels connected to detectors 15 and 16 were short source-detector channels. **b.** The sensitivity profiles obtained through 100 million photon simulations demonstrate the varying levels of sensitivity of the fNIRS source-detector probe configuration to cortical activation. The gradient scale depicts the regions where the probe was most sensitive (shown in red) and least sensitive (shown in blue).

Finally, a bandpass filter to the fNIRS data was applied to further remove motion-related noise, retaining frequencies between 0.01 Hz and 0.5 Hz. The modified Beer-Lambert Law (Delpy, 1988) was used to convert optical density units to HbO and HbR concentrations. A nuisance regressor was applied to each channel depending on which short source-detector channel was closest. The onset of each stimulus was convolved with a single gamma function, representing the canonical hemodynamic response. On each trial, a beta coefficient was calculated for HbO and HbR to reflect the amplitude of each signal every trial.

Preprocessing for image reconstruction

Next, channel-based time series data were converted to volumetric time series data (Forbes et al., 2021). The position of channels across participants invariably differs based on individual anatomy. Therefore, this approach provides better localization of activation by reconstructing individual brain atlases into a common brain, akin to the preprocessing steps in fMRI research.

NeuroDOT scripts in MATLAB were used to carry out the following steps. First, the data was converted to hemoglobin concentration values with a differential path-length factor of 6 for both wavelengths. The processed channel data was used to construct volumetric timeseries data based on the procedure outlined in Forbes et al. (2021). Colin's atlas was used that aligns each participant digitized anatomical landmarks into a standardized space. A light model was then created based on the digitized spatial coordinates. To create a sensitivity profile for each source-detector pair, photon migration simulations were performed using HOMER2's AtlasViewerGUI that simulates the photon migration path of near-infrared light emitting from each channel. Monte-Carlo simulations of 10,000,000 photons were simulated for each channel (Fang & Boas, 2009). Sensitivity profiles for each channel will be integrated to create a mask for each

participant that reflects the areas of the brain from which the fNIRS channels were recording. A mask at the group level was then created that included voxels in which at least 60% of participants had overlapping data.

Next, image reconstruction in NeuroDOT was used to combine the simulated light models with the channel time series data to create volumetric time-series data for each participant. Channel data were down-sampled from 25 Hz to 10 Hz to reduce computational demands. The Tikhonov regularization method was used to generate voxel time series data for HbO and HbR concentrations (Eggebrecht et al., 2014; Wheelock et al., 2019). Therefore, a simulated light model was combined with pre-processed channel data to produce volumetric timeseries data. Due to the complexity of accurately estimating near-infrared light diffusion in biological tissue, the Tikhonov regularization method (Wheelock et al., 2019) was used to generate voxel-wise timeseries data for each chromophore. This method helps to avoid rounding errors that could lead to an under-determined light diffusion solution. Once the reconstruction was complete, the amplitude of ΔHbO and ΔHbR for each condition per subject was estimated using a General Linear Model with a hemodynamic response function derived from diffuse optical tomography data (Forbes et al., 2021). The GLM consisted of several regressors to model the encoding event of each condition. These events were modelled using a 800 ms box-car function (equivalent to the encoding display duration) convolved with a gamma function (created using spm_Gpdf; h1 = 4, l1 = 0.0625; h2 = 12, l2 = 0.0625).

Statistical analyses

Behavioral analyses

The effects of set size (SS2, SS3, SS4, SS5) and trial type (same, different) on traditional outcome-based measures and continuous motor dynamics were assessed in the change detection

task. The following dependent variables were reported with a 2x4 repeated-measures ANOVA: Accuracy, RT, Pashler's K (Pashler, 1988; Rouder et al., 2011), area under the curve (AUC), and maximum deviation (MD) time (Freeman, 2014). VWM capacity was be assessed with Pashler's K. For each set size, Pashler's K was calculated to generate an index of VWM capacity. Pashler's K was extracted using Equation (1), in which *N* is the set size, *H* is the hit rate, *FA* is the false alarm rate, and *K* is the VWM capacity estimate.

$$K = N \times (H - FA) \quad (1)$$

AUC was examined as a measure of spatial attraction toward the incorrect response on each trial. AUC is calculated as the geometric area under each response trajectory and above the idealized response trajectory (i.e., the most linear path to the correct response location). AUC provides a holistic measure of how much participants deviate from the straightest possible path to the correct response location. In the context of the change detection task, higher AUC scores would indicate more deviation away from the correct response, or worse memory performance. MD time was also examined to better understand at what point in time the trajectory in each condition maximally deviates from the correct response. This measure indicates peak deviation along the x and y axis (i.e., the euclidean distance). For these analyses, only trajectories that maximally deviate toward the distractor response location were considered.

As a separate set of analyses, the time course of when participants began to move relatively closer to the target on same and different trials was examined. Typically, in change detection tasks a same response bias is found (e.g., Wijeakumar et al., 2017), in which accuracy is higher for same compared to different trials as set size increases. This result may be due to the increasing number of same items which activate the same response, while slowing down evidence accumulation for the different response. However, the specific time course of same vs.

different trial's decision making at varying set sizes is unclear. Traditional behavioral methods have used RT to evaluate the time of correct response initiation, but this approach provides limited insight, as RT scores only reflect the output and measurements can be similar across trials due to temporal differences in cognitive processes. For example, mouse-tracking studies have shown that velocity and acceleration changes across different points in trials can lead to similar RTs (see Kinder et al., 2022). To assess the timing at which target initiation occurs, the analysis procedure of Spivey (2005) was followed. First, trajectories x and y coordinates were averaged at each of the normalized 101-time steps. Next, the Euclidean distance to the target and distractor was calculated at each time point. In Equation (2), the Euclidean distance at a particular time is represented by d_{ij}, x_i and y_i denote the horizontal and vertical position at each

$$d_{ij} = \sqrt{\left(x_i - x_j\right)^2 + \left(y_i - y_j\right)^2} \quad (2)$$

time point, and x_j and y_j denote the horizontal and vertical position at either the target or distractor response location. For each set size, the divergence point at which same and different trials begin to move relatively closer to the target than the distractor was compared. For these analyses, an alpha of .006 was used as the threshold for statistical significance to control for multiple comparisons (Chen, 2017).

fNIRS analyses

The image reconstructed fNIRS data underwent a 4 (set size: SS2, SS3, SS4, & SS5) x 2 (change: same, different) x 2 (hemoglobin: HbO, HbR) repeated-measures ANOVA, which included correct trials only. The reconstructed fNIRS HbO and HbR maps were used for analysis with *3dMVM* in AFNI (Chen et al., 2014). The residuals for each voxel from the ANOVA were created and then used in AFNI's *3dClustSim* to determine the smallest cluster size required to

obtain a family-wise error rate of less than .05 and a voxel-wise threshold of less than .05 (Cox et al., 2017). Based on this approach, the minimum cluster size required was 21 voxels.

Behavioral results

In the following analyses, impact of set size and trial type (same or different) on conventional outcome-based measures (RT and accuracy) and mouse-tracking trajectory measures were examined. These analyses employed two-factor repeated measures ANOVAs. To address multiple comparisons, all pairwise comparisons were corrected using the Bonferroni-Holm correction. Finally, the time at which same and different trials diverge toward the target response location was examined for each set size to examine the same response bias.

Accuracy

There was a significant effect of trial type on accuracy, $F(1,34) = 16.26$, $p < .001$, $\eta_p^2 = .324$. Same trials ($M = 94\%$) had higher accuracy than different trials ($M = 88.4\%$), suggesting a bias toward the same response. There was also a significant effect of set size on accuracy, $F(3,102) = 74.26$, $p < .001$, $\eta_p^2 = .689$. As expected, accuracy decreased linearly as set size increased, $F(1,34) = 121.51$, $p < .001$, $\eta_p^2 = .781$. Pairwise comparisons showed that accuracy between SS2 ($M = 97.8\%$), SS3 ($M = 94.9\%$), SS4 ($M = 89.9\%$), and SS5 ($M = 83.1\%$) all significantly varied (all p's $< .05$). Finally, there was a significant set size x trial type interaction, $F(3,102) = 35.72$, $p < .001$, $\eta_p^2 = .512$. For set sizes 4 and 5, accuracy was significantly higher on same (SS4: $M = 92.2\%$, SS5: $M = 92.1\%$) than different trials (SS4: $M = 87.7\%$, SS5: $M = 74.1\%$), p's $< .01$. However, for set sizes 2 ($p = .282$) and 3 ($p = .332$), trial type had no effect on accuracy. This accuracy result suggests that the response bias toward same is present at higher set sizes (SS4 & SS5), but not present at lower set sizes (SS2 & SS3). These results can be seen in Figure 4a.

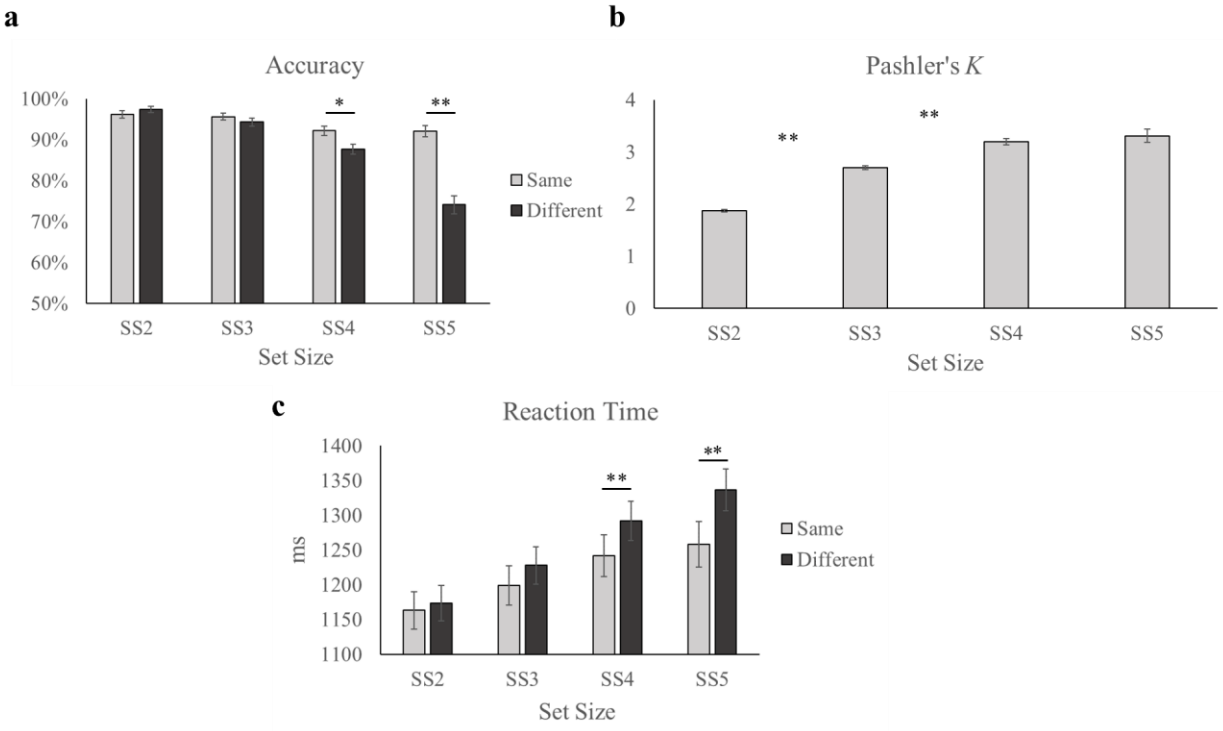

Figure 4. Experiment 1 Outcome-based Results. **a.** Accuracy plotted as a function of trial type and set size. **b.** Pashler's *K* plotted as a function of set size. **c.** Reaction time plotted as a function of trial type and set size. Error bars display SEM. * $p < .05$. ** $p < .01$.

Pashler's K

There was a significant effect of set size on VWM capacity estimates as measured by Pashler's *K*, $F(3,102) = 105.377$, $p < .001$, $\eta_p^2 = .756$. VWM capacity increased linearly as set size increased, $F(1,34) = 154.82$, $p < .001$, $\eta_p^2 = .820$. Pairwise comparisons showed that SS2 ($M = 1.87$) had a significantly lower *K* estimate than SS3 ($M = 2.69$), SS4 ($M = 3.19$), and SS5 ($M = 3.3$), all p's $< .001$. The only pairwise comparison that did not reach statistical significance was SS4 versus SS5, $p > .90$, which is consistent with previous findings that VWM capacity is approximately 4 items (Brady et al., 2011; Luck & Vogel, 2013). These results can be seen in Figure 4b.

Reaction time

There was a significant effect of trial type on reaction time (RT), $F(1,34) = 11.69$, $p = .002$, $\eta_p^2 = .256$. Same trials ($M = 1215.49$ ms) had significantly faster RTs than different trials ($M = 1257.47$ ms). There was also a significant effect of set size on RT, $F(3,102) = 36.16$, $p < .001$, $\eta_p^2 = .515$. RT slowed linearly as set size increased, $F(1,34) = 51.47$, $p < .001$, $\eta_p^2 = .602$. RTs between SS2 ($M = 1168.43$ ms), SS3 ($M = 1213.28$ ms), SS4 ($M = 1267.04$ ms), and SS5 ($M = 1297.16$ ms) all significantly differed (p's $< .001$), except for the pairwise comparison between SS4 and SS5 ($p = .150$). In addition, there was a significant trial type x set size interaction, $F(3,102) = 5.75$, $p = .001$, $\eta_p^2 = .145$. On SS4 and SS5, different trials (SS4: $M = 1292.07$ ms; SS5: $M = 1336.55$ ms) had significantly slower RTs than same trials (SS4: $M = 1242.01$ ms; SS5: $M = 1257.77$ ms), $p = .009$ and $p < .001$, respectively. RTs between same and different trials did not significantly differ on SS2 and SS3 trials, $p = .403$ and $p = .092$, respectively. These results (Figure 4c) followed the same pattern of results found with accuracy.

Area under the curve (AUC)

There was a significant effect of trial type on AUC, $F(1,34) = 4.96$, $p = .033$, $\eta_p^2 = .127$. Different trials ($M = .627$) had greater AUC than same trials ($M = .464$), suggesting a same response bias (i.e., greater curvature toward the same response on different trials). Next, there was a significant effect of set size on AUC, $F(3,102) = 3.10$, $p = .030$, $\eta_p^2 = .084$. Curvature was found to linearly increase as set size increased, $F(1,34) = 9.59$, $p = .004$, $\eta_p^2 = .220$. However, pairwise comparisons showed that curvature only significantly varied between SS2 ($M = .503$) and SS5 ($M = .583$), p = .025. There was no trial type x set size interaction effect, $F < 1$. Average trajectories broken down by trial type and set size can be seen in Figure 5a.

Maximum deviation time

A significant effect of trial type on MD time was found, $F(1,34) = 25.06$, $p < .001$, $\eta_p^2 = .424$. MD was reached at a significantly earlier point in time on same trials ($M = 585.64$ ms) than different trials ($M = 616.83$ ms) overall, suggesting that the bias toward the same response occurs during early processing. In addition, there was a significant effect of set size on MD time, $F(3,102) = 49.45$, $p < .001$, $\eta_p^2 = .593$. MD time increased linearly as set size increased, $F(1,34) = 66.36$, $p < .001$, $\eta_p^2 = .661$. Pairwise comparisons showed that MD time between SS2 ($M = 548.72$ ms), SS3 ($M = 580.58$ ms), SS4 ($M = 623.27$ ms), and SS5 ($M = 652.37$ ms) all significantly differed, p's $< .01$. Finally, there was also a significant trial type x set size interaction effect, $F(3,102) = 3.94$, $p = .01$, $\eta_p^2 = .104$. On same trials, MD time between SS4 and SS5 did not differ, $p = .114$ (all other p's $< .05$). The interaction effect was also driven by the difference between same and different trials MD time occurring later at higher set sizes. For example, at SS2, the mean difference between same and different trials MD time was 14.72 ms, whereas at SS5, the mean difference was 47.14 ms. Again, this result suggests that the same

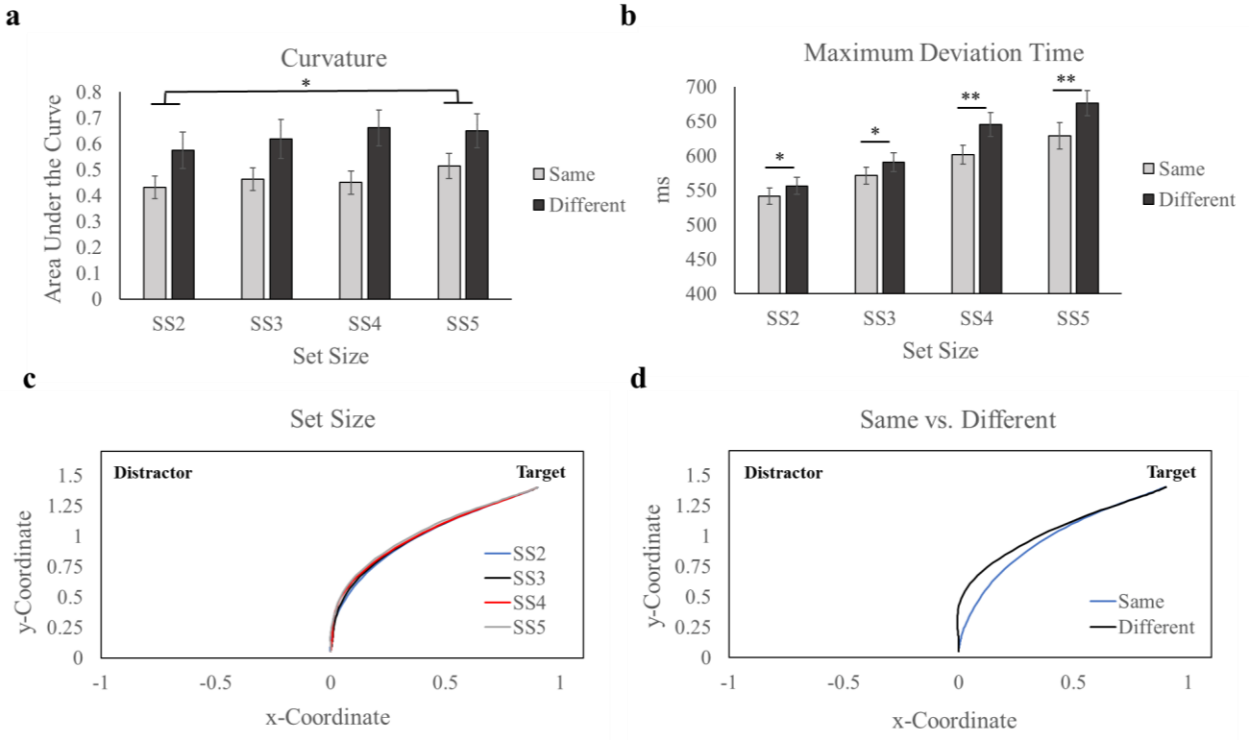

Figure 5. Experiment 1 Mouse-tracking Results. **a.** Curvature as measured with area under the curve plotted across conditions. **b.** Maximum deviation time plotted across conditions. **c.** Mean trajectories for each set size. d. Mean trajectories for each trial type. Error bars display SEM. * $p < .05$. ** $p < .01$.

response bias becomes stronger at higher set sizes. The MD time results can be seen in Figure 5b.

Same response bias

A "same response bias" is commonly found in change detection tasks, in which behavioral measures such as accuracy result in better performance on same trials than different trials (e.g., Wijeakumar et al., 2017). This effect tends to become stronger as set size increases (see Accuracy, RT, and MD time results above), suggesting that the presence of more same items biases response selection toward the same response. The following movement trajectory analyses were broken down by set size to examine the divergence point at which same and different trials began to move relatively closer to the target than the distractor location. As described earlier, the Euclidean distance, or proximity of the mouse-cursor to the target and distractor response locations over time was compared at each normalized time point. Figure 6 shows the Euclidean distance to the target and distractor for same and different trials. At the beginning of each trial, the proximity to the target and distractor response locations are similar due to the starting location being equidistant between the two. For SS2 (Figure 6a) same trials, target and distractor proximities begin to significantly diverge at the 35th normalized time step (p = .005; alpha = .006). On different trials, this divergence did not occur until the 45th normalized time step (p = .003). For SS3 (Figure 6b) same trials, divergence occurred at the 34th normalized time step (p = .004), compared to the 46th time step for different trials (p = .004). For SS4 (Figure 6c), same trials diverged at the 34th time point (p = .003) compared to the 48th time step for different trials (p = .005). Finally, for SS5 (Figure 6d), same trials diverged at the 35th time point (p = .005) compared to the 49th time point for different trials (p = .002).

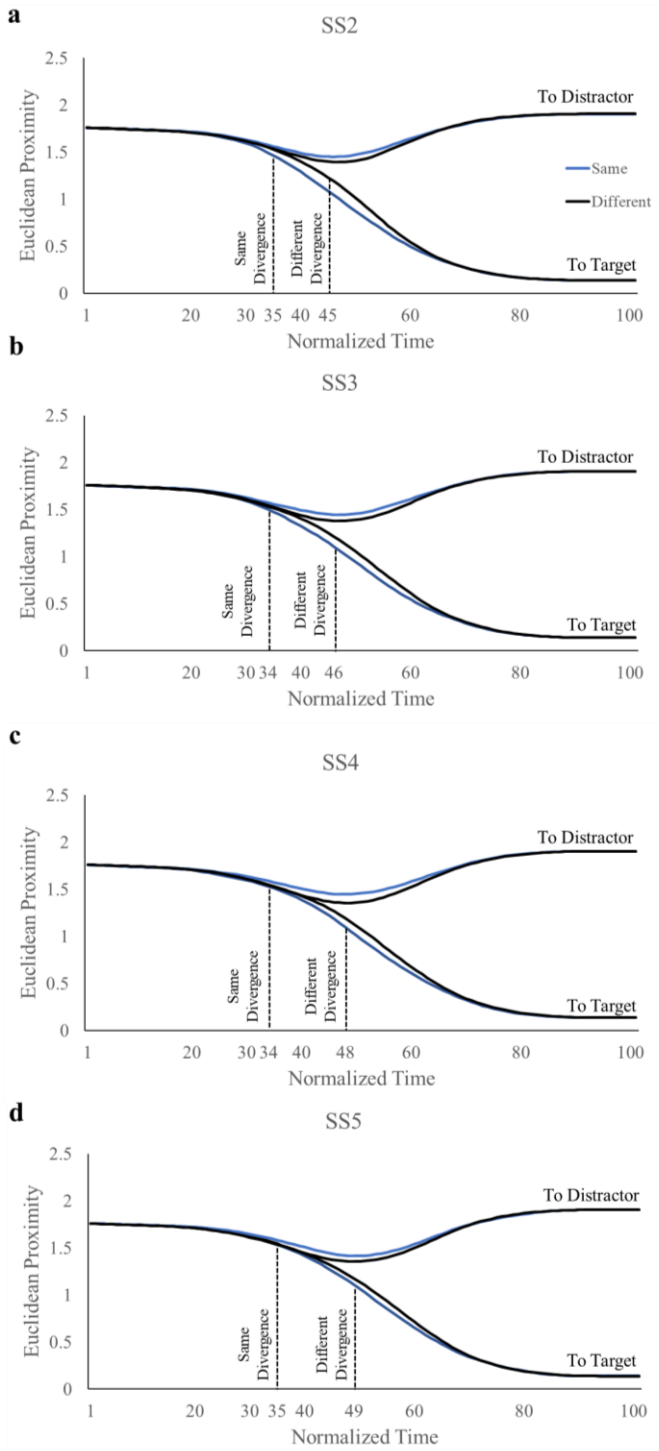

Figure 6. Euclidean Distance to the Target and Distractor across Conditions. Euclidean distances for same and different trials are shown for each set size, including the time at which significant divergences occurred (dashed lines; $p < .006$). **a.** SS2 trials **b.** SS3 trials **c.** SS4 trials. **d.** SS5 trials.

Overall, these findings strongly support a "same response bias" and shed light on its temporal dynamics. Across set sizes, same trials diverged sooner toward the target response location than different trials. There was also evidence that the same response bias becomes greater as set size increases, indicated by the difference between same and different divergences becoming greater at higher set sizes. For example, at SS2 there were 10 normalized time steps between same and different trials divergence points, but at SS4 there were 14 normalized time steps between these divergence points. Interestingly, same trials divergence points remained relatively constant across set sizes (SS2: 35th; SS3: 34th; SS4: 34th; SS5: 35th). This pattern of results suggests that the same response bias may not be driven by early, strong evidence accumulation on same trials. Rather, it may be that the same response bias is driven by slower evidence accumulation on different trials. Indeed, as set size increases, the divergence point on different trials occurs later (SS2: 45th; SS3: 46th; SS4: 48th; SS5: 49th). Due to the ratio of same-different items increasing on different trials as set size increases (e.g., 1:1 ratio at SS2; 3:1 ratio at SS4), early "same" response activation may slow and impair evidence accumulation on different trials (i.e., later divergences toward the target; also see MD Time results) and more errors (see Accuracy results above).

fNIRS results

To examine the impact of VWM demands on neural activity in the change detection task, the image-reconstructed fNIRS data were analyzed using AFNI's *3dMVM* with a repeated-measures ANOVA design that included set size (SS2, SS3, SS4, SS5), trial type (same, different), and hemoglobin (HbO, HbR) as factors. The analysis identified brain regions that showed significant main effects or interaction effects for clusters that exceeded the necessary cluster size threshold (i.e., a cluster containing a minimum of 21 voxels).

Group effects

The ANOVA revealed clusters in brain regions that were influenced by the independent variables of set size (SS2, SS3, SS4 & SS5) and change (same & different). Clusters were screened to only include those that interacted with hemoglobin (HbO & HbR). That is, only clusters in which HbO was greater than HbR were considered (indicating a meaningful change in neural activation; Kinder et al., 2022). These clusters and their associated effects are summarized in Table 3.

Frontal cortex. The first cluster in SFG revealed a significant main effect of hemoglobin, in which HbO (M = 0.61) was greater than HbR concentration (M = -.28), $t(34)$ = 2.58, p = .014 (Figure 7a), indicating that there was task-related activation in this region. In the IFG, there was a cluster showing a significant set size x change x hemoglobin interaction, $F(3, 102) = 3.98$, p = .010, η_p^2 = .105 (Figure 8c). The interaction effect was driven by HbO (M = .103) being greater than HbR (M = -.034) on SS4 different trials (p = .046). Further, HbO concentration significantly differed between same (M = -.046) and different trials for SS4, p = .009. This result suggests that IFG activation was associated with SS4, different trials in the change detection task.

Posterior parietal cortex. A cluster in the angular gyrus showed a significant set size x hemoglobin interaction effect, $F(3, 99) = 3.95$, p = .010, η_p^2 = .107 (Figure 7b). A simple main effect analysis showed that this interaction was driven by HbO (M = .217) being greater than HbR (M = -.087) concentration for SS4 trials, p = .035. This suggests that this region is active under high VWM demands, or when VWM is around capacity (~3-4 items). Further, HbO activation for SS4 was greater compared to SS3 (M = -.044), p = .04. Next, a cluster in the SPL

Table 3. Summary of significant fNIRS group effects in Experiment 1

Effect	Region	Cluster Size (# voxels)	MNI Coordinates (x, y, z)	*F* value
Hemoglobin	SFG	206	22, -4, 79	6.66*
SS x Hemoglobin	Angular gyrus	45	62, -62, 23	3.95*
Change x Hemoglobin	SPL	30	52, -48, 67	6.14*
SS x Change x Hemoglobin	IPL	44	50, -34, 63	3.01*
	IPL	30	58, -54, 53	3.67*
	IFG	25	50, 34, 31	3.98**

Note. * $p < .05$. ** $p < .01$.

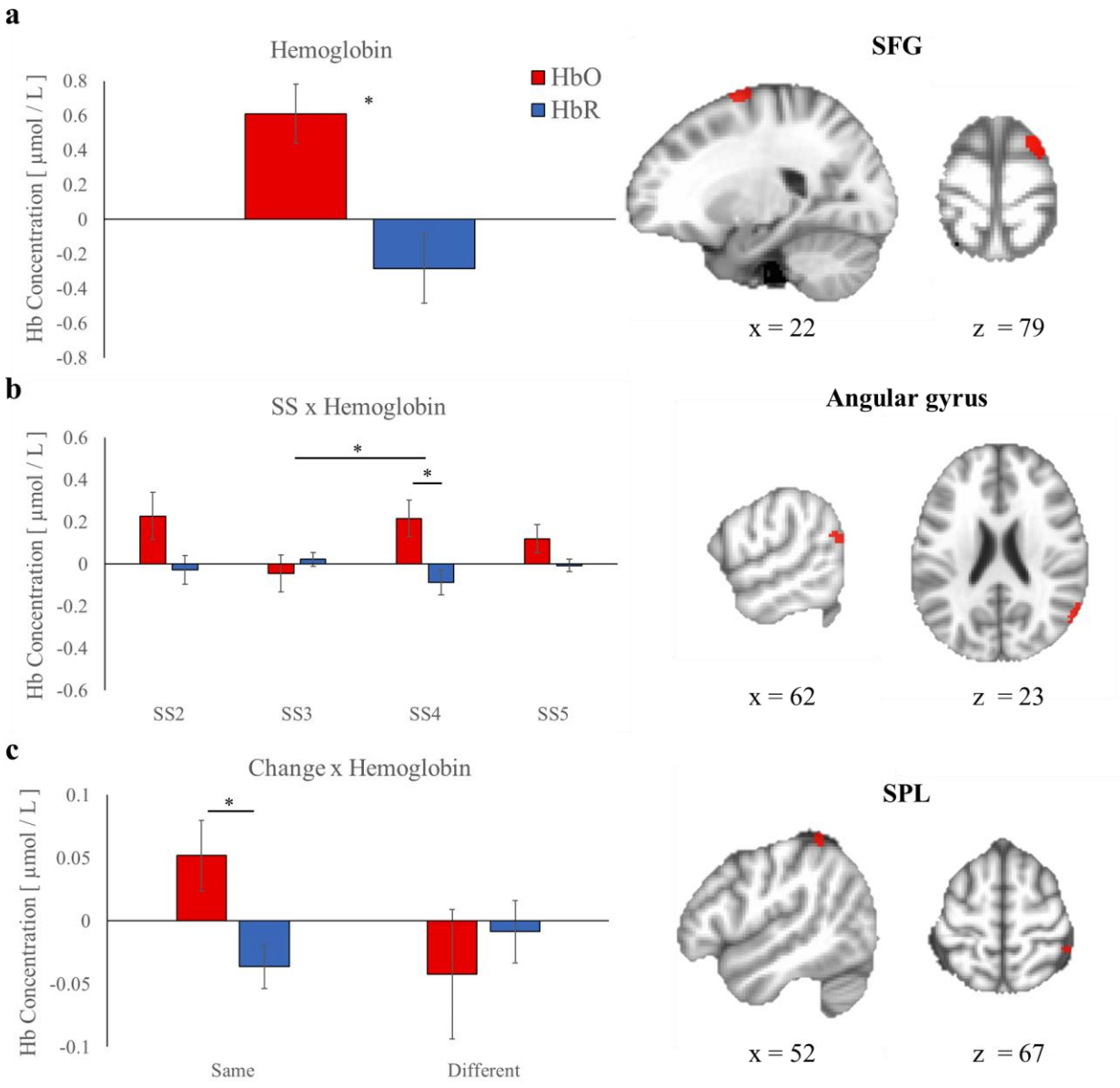

Figure 7. Experiment 1 fNIRS Main effects and Two-way Interactions. **a.** Main effect of hemoglobin in SFG. **b.** SS x hemoglobin interaction found in the angular gyrus. **c.** Change x hemoglobin interaction found in the SPL. Error bars display SEM. * $p < .05$.

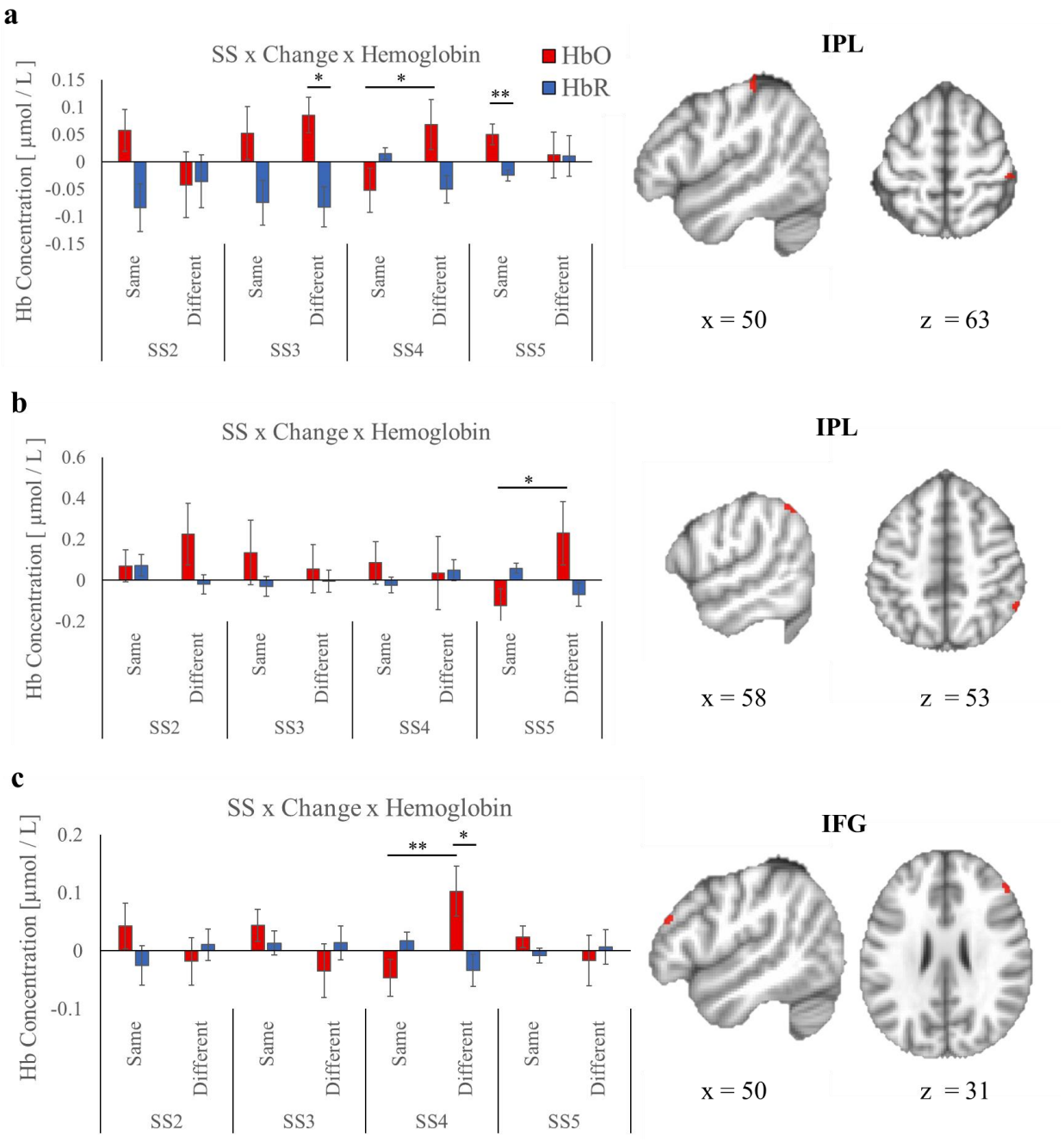

Figure 8. Experiment 1 fNIRS Three-way Interactions. **a.** SS x change x hemoglobin interaction effect in IPL. **b.** SS x change x hemoglobin interaction effect in another cluster in IPL. **c.** SS x change x hemoglobin interaction effect in IFG. Error bars display SEM. * $p < .05$. ** $p < .01$.

revealed a significant change x hemoglobin interaction, $F(1, 34) = 5.23$, $p = .029$, $\eta_p^2 = .133$ (Figure 7c). On same trials, HbO ($M = .052$) was greater than HbR ($M = -.036$), $p = .028$.

There were two clusters in the IPL that showed a significant set size x change x hemoglobin interaction (Figures 8a & 8b), $F(3, 96) = 3.01$, $p = .034$, $\eta_p^2 = .086$ and $F(3, 102) = 3.69$, $p = .014$, $\eta_p^2 = .098$, respectively . In the first IPL cluster (Figure 8a), HbO ($M = .085$) was greater than HbR ($M = -.083$) on SS3, different trials, $p = .016$. In addition, HbO ($M = .05$) was greater than HbR ($M = -.025$) on SS5, same trials, $p = .007$. Lastly, this cluster also showed greater activation for SS4 different trials ($M = .068$) compared to SS4 same trials ($M = -.052$), $p = .027$. This result shows that this region is engaged on different trials at or near VWM capacity (SS3 & SS4), but not outside of capacity (SS5). The second IPL cluster (Figure 8b) showed greater HbO concentration for SS5 different ($M = .230$) compared to same trials ($M = -.124$). However, HbO was not significantly greater than HbR in the SS5, different condition, $p = .137$.

fNIRS and behavioral correlations

The relationship between neural and mouse-tracking measures was assessed through bivariate correlation analyses with AFNI's *3dttest+* function and in SPSS. Voxel-wise residuals from each correlation analysis were used to estimate the minimum cluster size to achieve significance ($p < .05$). Beta weights from the significant correlation clusters were extracted and analyzed to determine the Pearson Correlation Coefficient and for visual inspection. For each set size and trial type, AUC was correlated with activation in clusters in which HbO was greater than HbR. These clusters and their behavioral correlations are summarized in Table 4.

Same trials

Frontal cortex. There was a strong negative correlation between AUC and HbO concentration in a cluster in IFG on SS2 trials ($r = -.503$, $p = .002$; Figure 8a), indicating that as

Table 4. Correlations between AUC scores and fNIRS data in Experiment 1

Condition	Region	Cluster Size (# voxels)	MNI Coordinates (x, y, z)	*r* value
SS2 Same	IFG	113	60, 12, 19	-.503**
	SMA	57	8, 28, 67	.462**
	SFG	33	24, 38, 51	-.454**
SS3 Same	Precentral gyrus	135	24, -18, 77	-.450**
	Angular gyrus	33	44, -78, 39	.514**
SS5 Same	IPL	118	52, -38, 55	.398*
SS2 Different	SPL	69	40, -50, 69	.440**
	MFG	26	44, 30, 35	.418**
SS3 Different	SFG	57	16, 2, 75	.418*
	MFG	29	36, 46, 37	.381*
SS5 Different	Precentral gyrus	112	46, 6, 53	-.485**
	MFG	67	44, 28, 41	.464**

Note. * $p < .05$. ** $p < .01$.

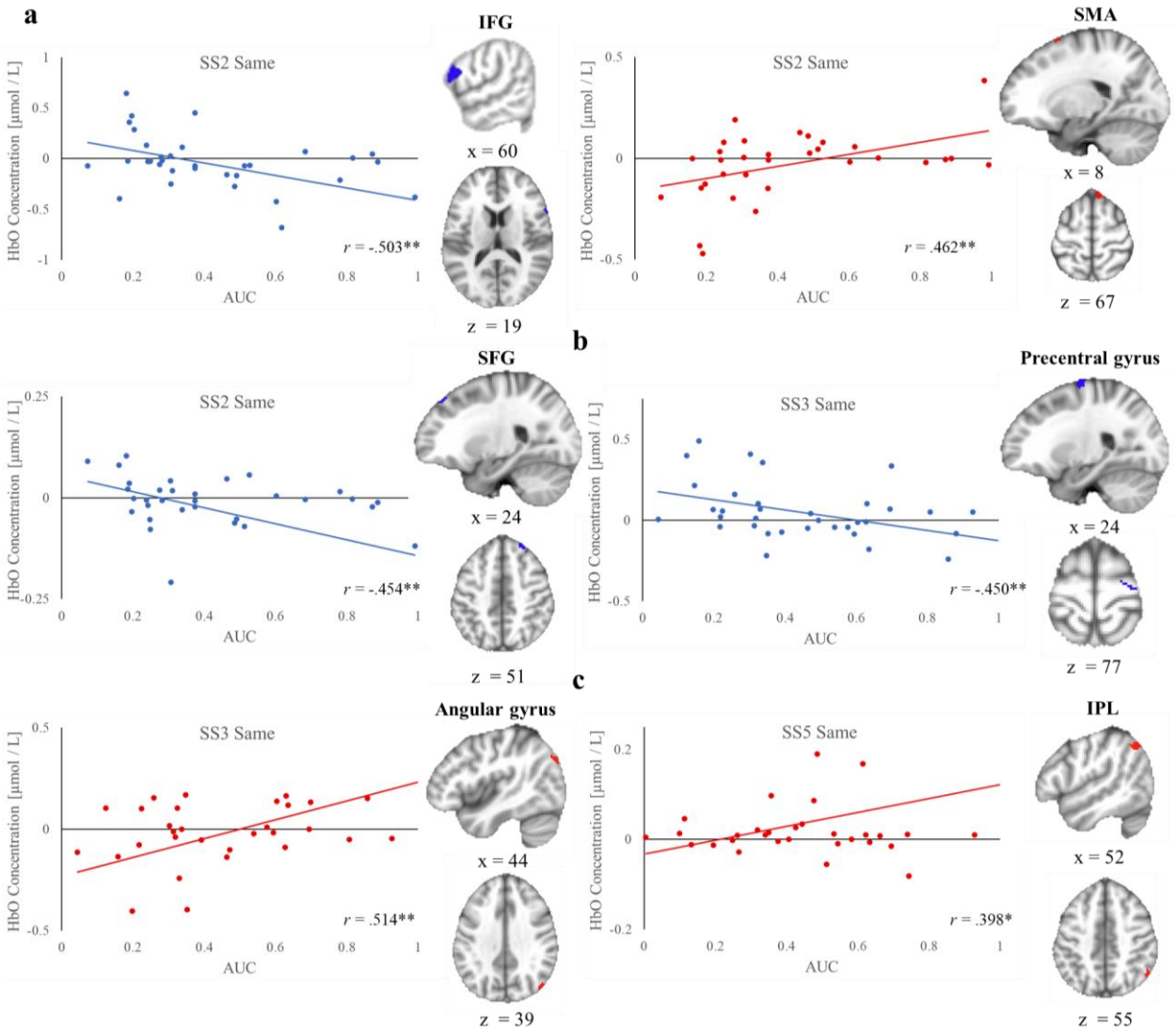

Figure 8. Experiment 1 fNIRS and AUC Correlations for Same Trials. **a.** SS2 same trials correlations. **b.** SS3 same trials correlations. **c.** SS5 same trials correlations. * $p < .05$. ** $p < .01$.

activation increased, performance improved (i.e., less curvature or a more direct path toward the target response). Similarly, there was a negative correlation between AUC and HbO concentration on SS2 trials in SFG (r = .479, p = .004; Figure 8a).

Motor cortex. There was a positive correlation between AUC and HbO concentration in the SMA on SS2 trials (r = .462, p < .008; Figure 8a), suggesting that performance worsened (i.e., more curvature away from the target response) as activation increased in this cluster. Conversely, in the precentral gyrus, there was a cluster showing a moderately strong negative correlation between AUC and HbO concentration on SS3 trials (r = -.450, p = .007; Figure 8b).

Posterior parietal cortex. There was a cluster in the angular gyrus showing a significant negative association between AUC and HbO concentration on SS3 trials (r = .450, p = .007; Figure 8b). On SS5 same trials, there was a positive correlation between AUC and HbO in a cluster in the IPL (r = .398, p = .018; Figure 8c).

Different trials

Frontal cortex. There were three clusters in MFG related to behavioral performance on SS2, SS3, and SS5 trials (Figure 9a-c). On SS2 trials, MFG showed a positive correlation between AUC and HbO (r = .418, p = .013). Similarly, On SS3 and SS5 trials, MFG showed a positive correlation (r = .381, p =.029 & r = .464, p = .005 respectively). On SS3 trials, there was also a positive correlation between AUC and HbO in a cluster in SFG (r = .418, p = .013; Figure 9b).

Motor cortex. There was one cluster in motor cortex that was found to predict behavioral performance. On SS5 trials, precentral gyrus showed a negative correlation between AUC and HbO (r = .485, p = .003; Figure 9c).

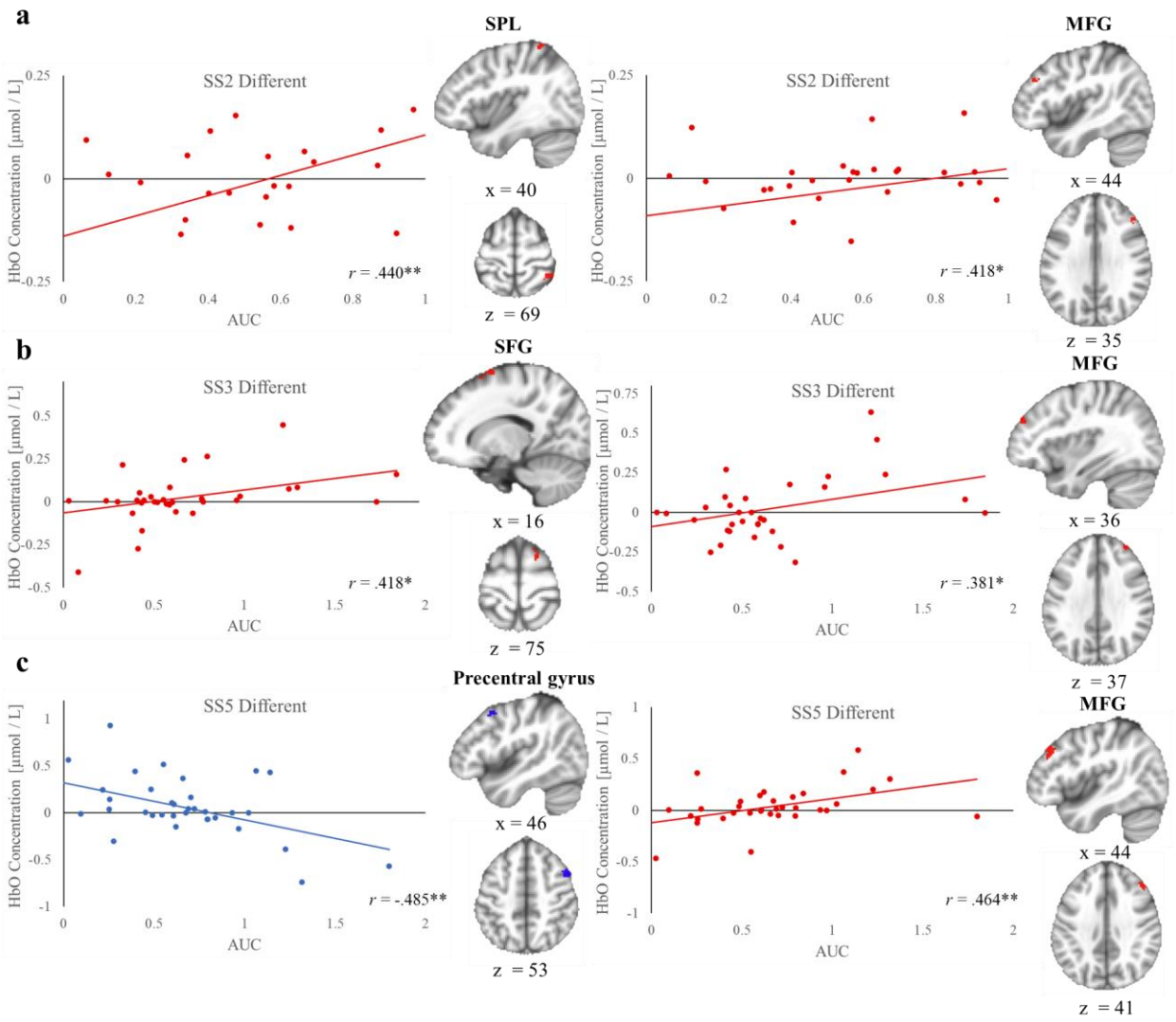

Figure 9. Experiment 1 fNIRS and AUC Correlations for Different Trials**. a.** SS2 different trials correlations. **b.** SS3 different trials correlations. **c.** SS5 different trials correlations. * $p < .05$. ** $p < .01$.

Posterior parietal cortex. There was one cluster in posterior parietal cortex that showed an association with behavioral performance. In the SPL, HbO concentration was positively correlated with AUC on SS2 trials (r = .440, p = .008; Figure 9a).

Chapter 3: Experiment 2

The results of Experiment 1 demonstrated that mouse-tracking measures, which capture behavior over time, can be utilized to better understand VWM performance. Response curvature was also found to relate to activity in regions of interest that are commonly implicated in the VWM frontoparietal network, including IPL, SPL, MFG, and SFG (Linden et al., 2003; Pessoa & Ungerleider, 2004; Todd & Marois, 2004; Wijeakumar et al., 2017). After establishing that mouse-tracking measures predict VWM performance, in Experiment 2 the primary aim was to examine the effect of action on VWM encoding. To do this, I manipulated action during VWM encoding in the change detection task. Specifically, participants either executed a task-relevant response (active move), a task-irrelevant response (passive move), or no response during encoding. I hypothesized that task-relevant actions would enhance VWM encoding compared to no movement, in line with the findings of my previous work on long-term memory encoding (Kinder & Buss, 2021).

Methodology

Participants

Participants included undergraduate students (29 female) ranging from 18-23 years of age from the University of Tennessee, Knoxville. Three participants were dropped because they had poor key press encoding accuracy (more than 2 standard deviations below the group mean; 73.42%) in the active and passive motor versions of the change detection tasks (46.25%, 52.50, and 42.50% key press accuracies). One additional participant was dropped due to not following task instructions, resulting in low shape change detection performance (61.3%), which fell more than two standard deviations below the group mean (82.1%). As a result, the final sample size for Experiment 2's results consisted of 32 participants. Participants provided informed consent,

completed a demographics survey upon arrival, and were compensated with course credit upon completion of the study. The University of Tennessee Institutional Review Board approved the proposed study's protocols.

Apparatus and stimuli

The set-up was identical to Experiment 1 with the following exception: 1) Either colored circles or triangles were randomly selected on each trial to be presented during the encoding display. Participants performed the change detection tasks on a computer monitor with a resolution of 1920 x 1080 pixels and a refresh rate of 60Hz while sitting approximately 60 cm away from the screen. MouseTracker and MATLAB R2022a software were used to present stimuli and record participants' mouse movements at a sampling rate of 60Hz. Each trial began with a "Start" button click and a fixation cross appearing on the screen. Response locations and stimuli were displayed on a uniform gray background. The colored circles or triangles were randomly selected from a pool of six colors that were at least 60º apart in color space and were presented along positions of an imaginary circle separated by at least 60º.

Design and procedure

The basic structure of the change detection tasks is shown in Figure 10. In alternating blocks, participants performed either a "no move" (Figure 10a), an “active move" (Figure 10b), or a “passive move” (Figure 10c) change detection task. The sequencing of tasks was randomly generated at the start of each experiment. Participants completed 6 blocks (two for each task) with 40 trials presented in each task block. Participants also completed three blocks of practice trials (10 trials in each block) for each task at the start of the experiment. The order of the practice blocks was randomly generated. An example sequence of each change detection task was shown at the start of the experiment.

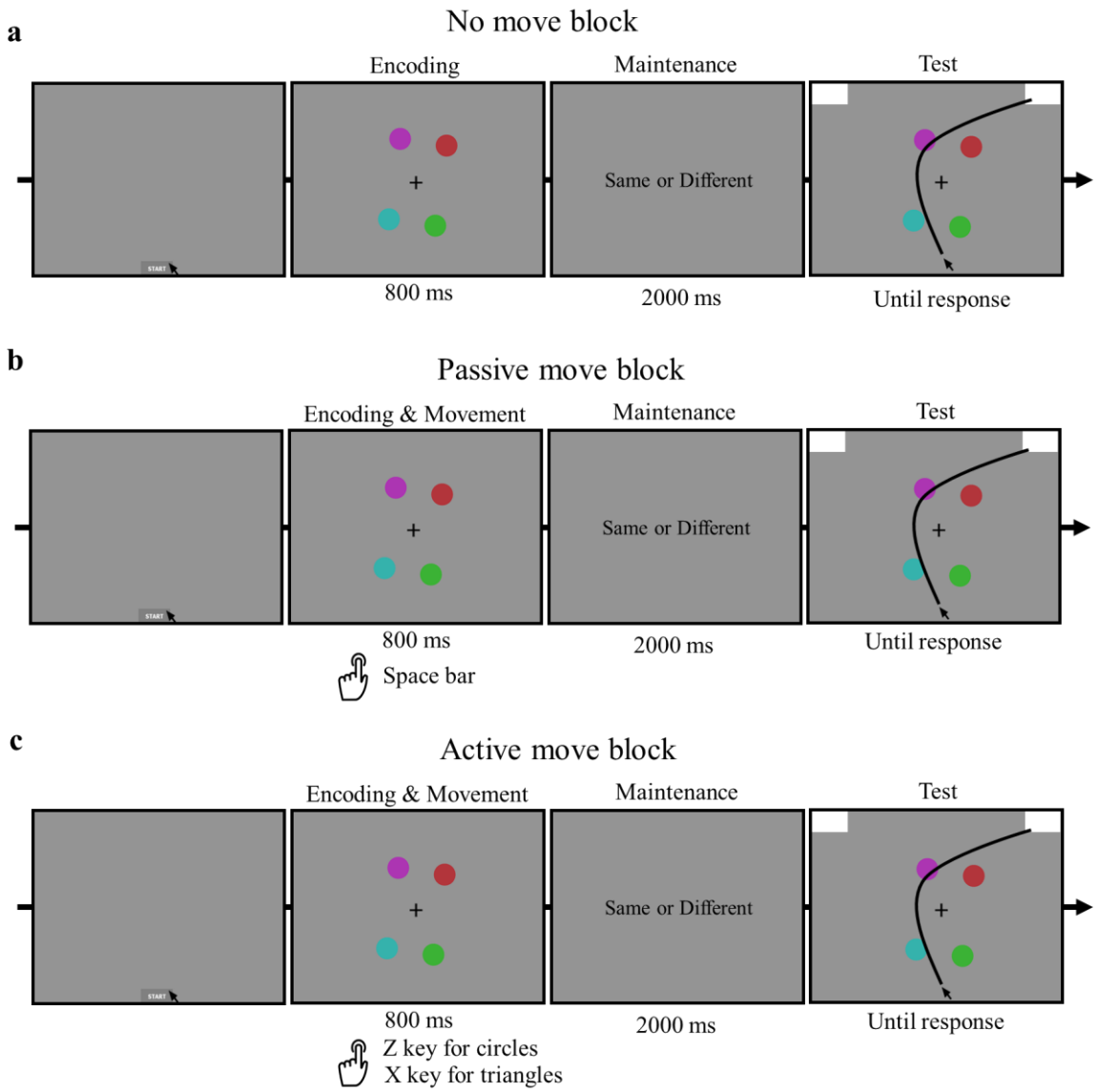

Figure 10. Experiment 2 Change Detection Tasks. **a.** In the no move change detection task, an encoding array briefly appears, followed by a maintenance interval and a test array. On "same" trials, the colors and the shapes during the test array are identical to those in the encoding array. On "different" trials, either one of the colors changes, or all the shapes change during the test array compared to the encoding array. **b.** The passive move change detection task is identical to the no move version, except participants execute a space bar button-press during the encoding array. **c.** In the active move change detection task, participants instead make a shape judgement response during the encoding array.

No move change detection task

Each trial began when participants clicked the "Start" button, followed by a fixation cross presented for 500 ms at the center of the screen. Then, the encoding display was presented for 800 ms, immediately followed by a 2000 ms maintenance interval. During the maintenance interval, the text "Same or Different" in 12 size font was presented at the center of the screen. Participants were tasked to remember the color and shape of the four items that appeared during the encoding display. During the test display, a same or different trial type will occur. For same trials, the colors and shapes of all stimuli on the test display remained the same as they had appeared on the encoding display. For different trials, either one of the item's color will change, or all of the shapes will change (e.g., circles to triangles) for the test display compared to the encoding display. Same and different responses were mapped to the upper-left and upper-right response locations (counterbalanced across participants). The mouse cursor was locked at the Start location until the onset of the test display. Participants were instructed to initiate moving the mouse cursor as quickly as possible once the test display appeared. A minimum intertrial interval was set to 500ms.

Trial type trials (same & different) were randomly intermixed across the two blocks of the no move change detection task, with 40 trials in each block. In different trial type trials, the color changed 80% of the time (32 trials), and the shapes changed 20% of the time (8 trials). Shape change trials were used to ensure participants would also attend and encode the shape of the stimuli in the array, which would be held constant and manipulated in the following move versions of the change detection tasks.

Passive move change detection task

The passive move version of the change detection task was identical to the no move change detection task, except that participants initiated a task-irrelevant motor movement during the encoding display of the task. Specifically, on every trial, participants pressed the space bar when the encoding display appeared. Participants were instructed to respond as quickly as possible when the encoding display appeared (i.e., the movement was associated with the encoding display onset, not the stimuli). The encoding display lasted for 800 ms, followed by a 2000 ms maintenance interval, and finally the test display appeared until a same/different response occurred. The sequence of events in the passive move version of the change detection task can be seen in Figure 10b. As in the no-move version of the change detection task, trial types (same & different) were randomly intermixed across the two blocks of the passive move change detection task. On different trials, the color changed 80% of the time (32 trials), and the shape changed 20% of the time (8 trials).

Active move change detection task

The active move version of the change detection task was identical to the no move change detection task, with the exception that participants executed a task-relevant motor movement during the encoding display. In addition to encoding the items into VWM, participants were instructed to make a shape judgment of the stimuli in the display. Depending on whether the shapes of the items are all circles or triangles, participants pressed either the "z" or "x" key (key to shape mappings were counterbalanced across participants) with their left hand. Participants were instructed to respond with a shape judgement key press as quickly and as accurately as possible. After participants make a circle or triangle response and the encoding display offsets (800 ms), the maintenance interval occurred (2000 ms), followed by the test

display (until response; Figure 10c). The active move change detection task consisted of two blocks, and the trial types (same and different) were randomly intermixed throughout. The color changed in 80% of the different trials (32 trials; action-irrelevant), while the shape changed in 20% of the different trials (8 trials; action-relevant).

Mouse-tracking methods

Data preprocessing

Movement trajectory preprocessing and exclusion criteria were the same as in Experiment 1, with the exception that trials in the movement change detection task were discarded if an incorrect movement was executed (if any) during the encoding display.

Movement trajectories along the x- and y-axes were transformed into a standard coordinate space, with trajectories to the left response location remapped to the right location to overlay all trajectories to the same response location. Trajectories were normalized into 101-time steps for spatial data preprocessing to compare trials of varying response times. After spatial normalization, x and y coordinates were averaged for each participant.

The same trial exclusion criteria were used as in Experiment 1, with the exception that incorrect movement responses in the passive and active movement blocks and incorrect shape change trials were also excluded. Trials that were excluded from analyses included incorrect test trials (13.73% of trials), trials with slow reaction times (3.91% of trials), trials with slow movement initiations (3.22% of trials), trials with abnormal trajectories (6.42% of trials), and incorrect key presses in the movement blocks (7.7% of trials). In total, 23.98% of trials were excluded from subsequent analyses not related to accuracy.

Statistical analyses

Behavioral analyses

The impact of trial type (same, different) and movement (no move, passive move, active move) on both conventional outcome-based measures and continuous motor dynamics were evaluated in the change detection task. A 2x3 repeated-measures ANOVA was used to examine the same behavioral dependent variables as in Experiment 1, including Accuracy, RT, Pashler's K, AUC, and MD time. To control for multiple comparisons, the Bonferroni-Holm correction was applied to all pairwise comparisons.

Behavioral results

Movement encoding accuracy

Movement encoding accuracy in the passive and active move blocks was analyzed in two ways: 1) accurate responses regardless of timing, and 2) accurate responses that occurred during the encoding display (i.e., encoding movement accuracy within 800 ms). The first analysis examined whether participants are following task instructions. For this analysis, overall accuracy was 89.90%. Overall accuracy was significantly higher in the passive move task (M = 94.45%) than in the active move task (M = 85.35%), $t(31) = 5.88$, $p < .001$. Next, encoding movement accuracy overall was 83.77%. Encoding movement accuracy was significantly higher in the passive movement task (M = 89.02%) than in the active movement task (M = 78.52%), $t(31) = 6.06$, $p < .001$. These results suggest that, as expected, the active movement task was more difficult than the passive movement task due to the movement being tied to specific features (the shapes) of the stimuli.

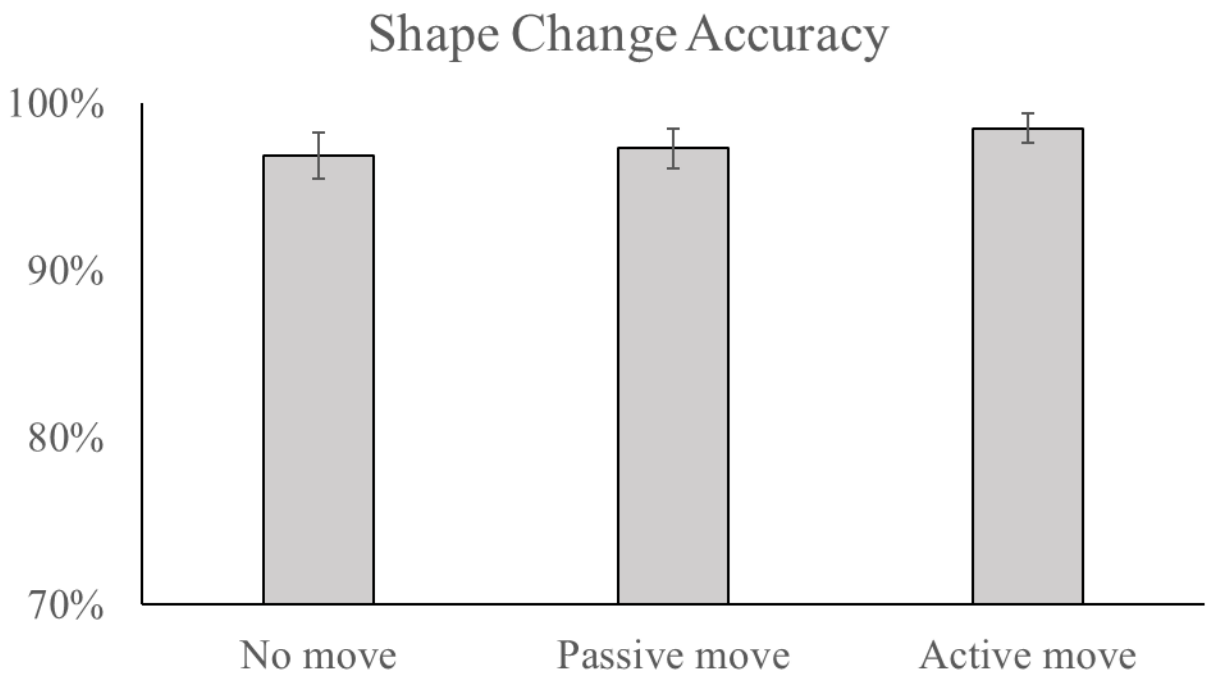

Figure 11. Experiment 2 Shape Change Accuracy Results. Error bars display SEM.

Shape change detection accuracy

Overall, shape change accuracy was very high across conditions (M = 97.5%; Figure 11). There was no effect of movement on shape change detection accuracy, $F < 1$. No move (M = 96.9%), passive move (M = 97.3%), and active move (M = 98.5) trials did not differ, p's > .90.

Overall change detection accuracy

There was no effect of trial type (same, different) or movement on accuracy, $F < 1$. However, there was a significant trial type x movement interaction, $F(2,62) = 4.16$, p =.020, η_p^2 = .118. A simple main effect analysis showed that on active move trials, accuracy was significantly higher for same (M = 87.4%) compared to different trials (M = 80.1%). These results can be seen in Figure 12a.

Pashler's K

There was no significant effect of movement on VWM capacity estimates as measured with Pasher's K, F = 1.54. No move (M = 2.83), passive move (M = 2.70), and active move (M = 2.70) trials did not differ (Figure 12b).

Reaction time

There was no effect of trial type on RT, $F < 1$. There was a significant effect of movement on RT, $F(2,62) = 3.63$, p =.032, η_p^2 = .105. No move trials (M = 1418.63 ms) had significantly slower RTs than passive move trials (M = 1367. 88), p = .013. No move trials RTs did not differ from active move trials (M = 1391.98 ms), p = .807, and there was no difference between passive move and active move trials, p = .366. The trial type x movement interaction effect was not significant, $F < 1$. A breakdown of RT scores can be seen in Figure 12c.

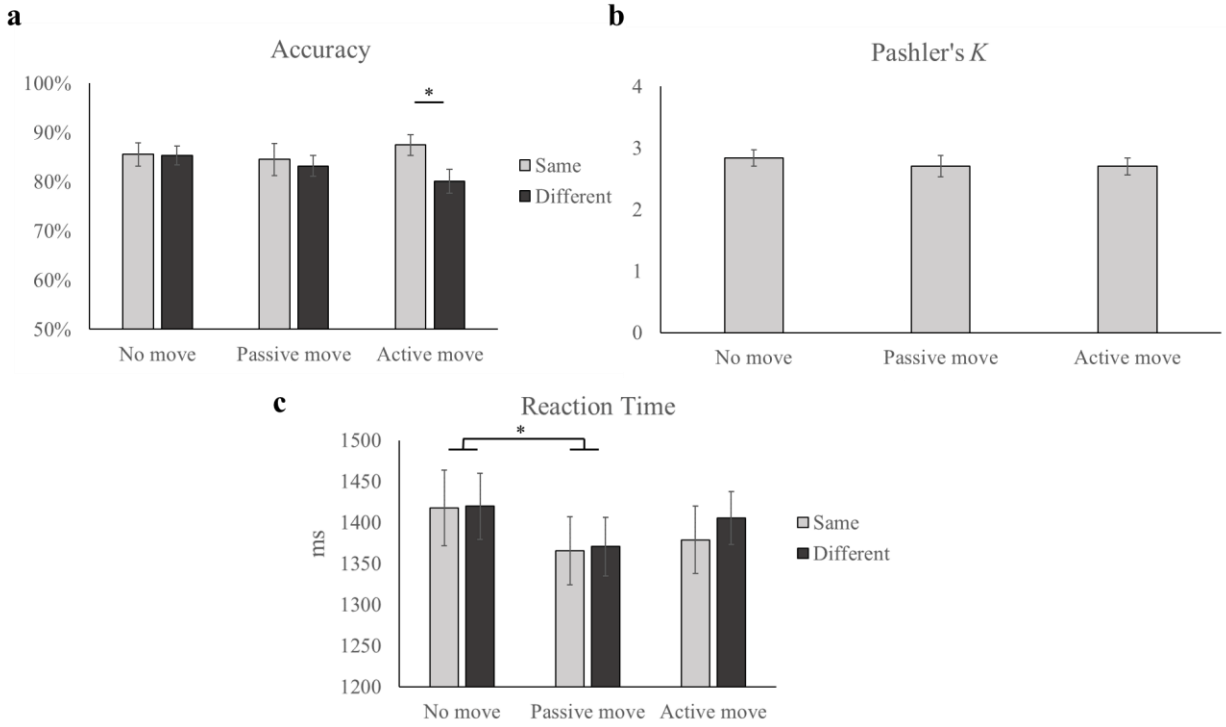

Figure 12. Experiment 2 Outcome-based Results. **a.** Accuracy plotted as a function of trial type and movement. **b.** Pashler's *K* plotted as a function of movement. **c.** Reaction time plotted as a function of trial type and movement. Error bars display SEM. * $p < .05$.

Area under the curve

There was no significant effect of trial type or movement on AUC scores (Figure 13a), $F < 1$. The trial type x movement interaction was also non-significant, $F = 1.39$. Average trajectories broken down by trial type and movement conditions can be seen in Figure 13 c-d.

Maximum deviation time

There was no significant effect of trial type on MD time, $F < 1$. The effect of movement on MD time reached marginal significance, $F(2,62) = 2.92$, $p = .061$, $\eta_p^2 = .086$. MD time on no move trials ($M = 693.02$ ms) occurred marginally later compared to passive move trials ($M = 662.41$ ms), $p = .060$. The trial type x movement interaction did not reach significance, $F < 1$. A breakdown of MD time measures for Experiment 2 can be seen in Figure 13b.

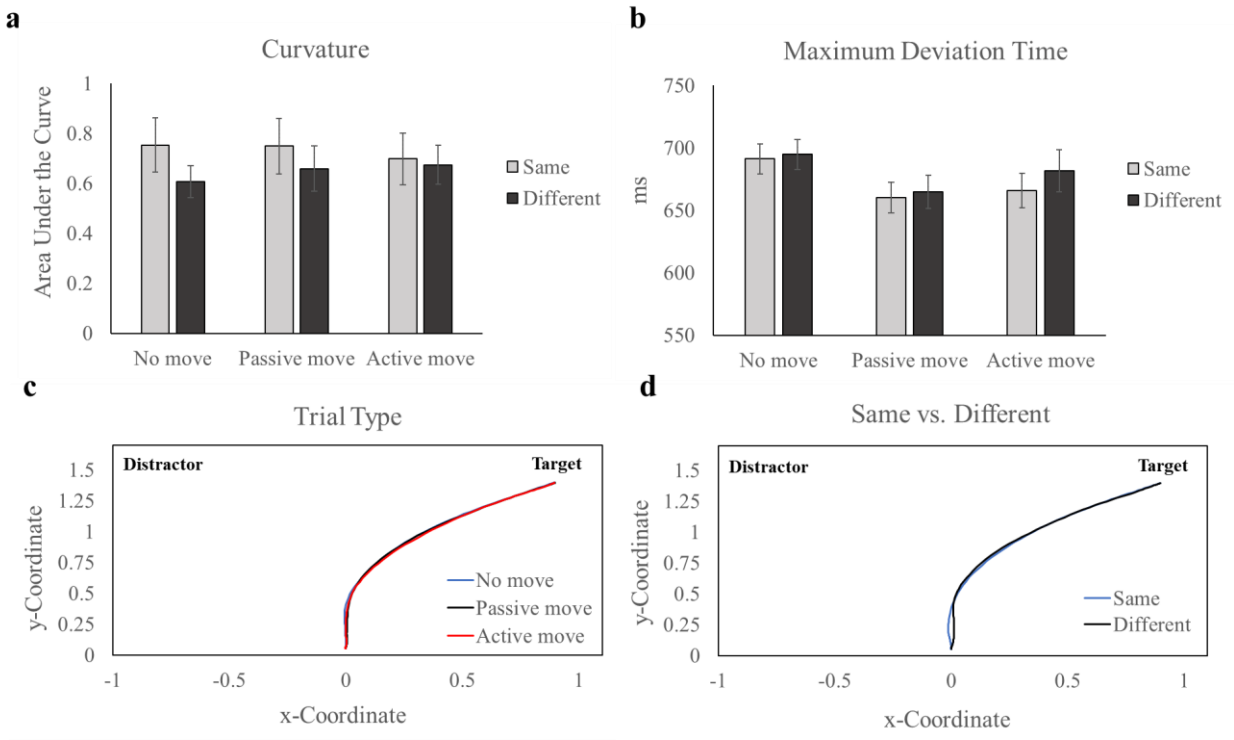

Figure 13. Experiment 2 Mouse-tracking Results. **a.** AUC plotted across conditions. **b.** MD time plotted across conditions. **c.** Mean trajectories for each movement type in the change detection task. **d.** Mean trajectories for each trial type. Error bars display SEM.

Chapter 4: Experiment 3

Experiment 2 investigated the effect of action on VWM encoding with a mouse-tracking paradigm. The results indicated that neither task-relevant (active move) nor task-irrelevant (passive move) actions influenced VWM encoding. However, it is possible that the complex design of three alternating tasks introduced additional task demands that negatively impacted the movement change detection tasks, as evidenced by the surprisingly low movement accuracy during encoding in the passive and move blocks. In order to address this issue, Experiment 3 simplified the design by using only two alternating tasks and focused on comparing the active move and no move change detection tasks, similar to the design in my previous work (Kinder et al., 2021). Furthermore, fNIRS was employed in Experiment 3 to explore the brain-behavior relationships between VWM performance, as measured by response curvature, and action during VWM encoding.

Methodology

Participants

Experiment 3 consisted of 36 participants (32 female; 18-22 years of age), all of whom were undergraduate students at the University of Tennessee, Knoxville. One participant was dropped because they had low movement encoding accuracy (68%) in the active move block (more than 2 standard deviations below the group mean; 74.9%). Two more participants were dropped because they had poor shape change detection accuracy (10% and 20%) in the no move block (more than 2 standard deviations below the group mean; 49.0%). One additional participant was dropped because the fNIRS cap was unable to make contact and record from the scalp. After these exclusions, the final sample size consisted of 32 participants. Prior to the study, participants provided informed consent and completed a demographics survey. Upon

completion, participants were compensated with course credit. The study's protocols were approved by the University of Tennessee Institutional Review Board.

Apparatus and stimuli

The set-up was identical to Experiment 2. Participants completed the change detection tasks on a computer monitor with a resolution of 1920 x 1080 pixels and a refresh rate of 60Hz, while seated approximately 60 cm away from the screen. Stimuli presentation and mouse movement recording were carried out using MATLAB R2022a and the MouseTracker software at a sampling rate of 60Hz. Each trial began with a "Start" button click and a fixation cross displayed on a uniform gray background. Stimuli were presented on an imaginary circle separated by at least 60º, and the colored circles or triangles were randomly selected from a pool of six colors that were at least 60º apart in color space.

Design and procedure

Figure 14 illustrates the basic structure of the change detection tasks. At the start of the experiment, participants alternated between performing a no move (Figure 14a) and an active move (Figure 14b) change detection task in randomly generated sequencing. Each experiment consisted of 4 blocks, with 50 trials presented in each task block, totaling 200 trials. Participants completed two practice blocks of each task, consisting of 10 trials each, at the start of the experiment. The order of the practice blocks was also randomly generated, and participants were provided with an example sequence of each change detection task at the start of the experiment.

No move change detection task

The no move change detection task was the same as in Experiment 2. At the beginning of each trial, participants clicked the "Start" button and viewed a fixation cross presented at the center of the screen for 500 ms. This was followed by an encoding display shown for 800 ms and

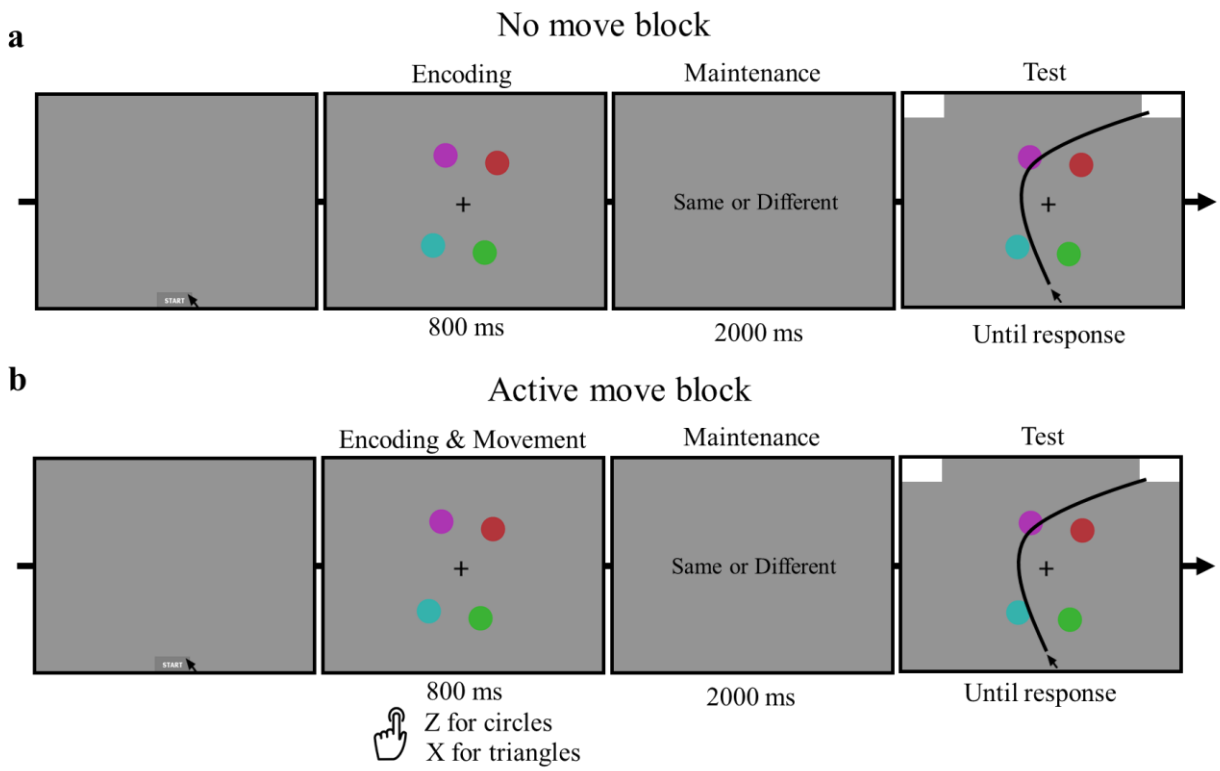

Figure 14. Experiment 3 Change Detection Tasks. Trial sequence for the no move (**a.**) and active move (**b.**) change detection tasks in Experiment 3, identical to those used in Experiment 2.

then a 2000 ms maintenance interval. Participants were instructed to remember the color and shape of the four items shown during the encoding display. Next, a same or different test display occurred. On same trials, the test display items had the same colors and shapes as those in the encoding display, while on different trials, the color of one item or the shapes of all items were altered. Same and different responses were assigned to the upper-left and upper-right response locations, which were counterbalanced across participants. The mouse cursor was fixed at the Start location until the onset of the test display. Participants were asked to initiate moving the mouse cursor as soon as possible after the test display appeared. A minimum intertrial interval of 500 ms was implemented.

In the no move change detection task, trial types (same and different) were randomly presented in two blocks of 50 trials each. On different trials, the color changed in 80% of the trials (40 trials), while the shape changed in 20% of the trials (10 trials). Similar to Experiment 2, shape change trials were included to ensure participants attended and remembered the shape of the stimuli, as in the active move block.

Active move change detection task

The active move change detection task used in Experiment 2 was replicated here. Participants used the "z" or "x" key with their left hand to respond based on whether the shapes of the items were circles or triangles, respectively. Participants were instructed to respond quickly and accurately. After the encoding display (800 ms), the maintenance interval occurred (2000 ms), followed by the test display (displayed until response). The active move task consisted of two blocks, with same and different trials randomly intermixed. On different trials, the color changed 80% of the time (40 trials; action-irrelevant) and the shapes changed 20% of the time (10 trials; action-relevant).

Mouse-tracking methods

Data preprocessing

Mouse-tracking preprocessing and exclusion criteria were the same as those used in Experiment 2. The movement trajectories along the x- and y-axes were converted to a standard coordinate space. Trajectories that went to the left response location were remapped to the right location to align all trajectories to the same response location. The trajectories were then normalized into 101-time steps to compare trials with different response times. Following spatial normalization, the x and y coordinates were averaged for each participant.

Trials that were excluded from subsequent analyses comprised of incorrect change detection test trials (15.21%), trials with slow times (4.24%), trials with slow movement initiations (2.44%), trials with abnormal trajectories (6.72%), and incorrect key presses in the movement block (8.19%). Overall, 25.6% of trials were excluded from subsequent analyses, not including accuracy analyses.

fNIRS methods

Data acquisition and probe design

The same fNIRS probe design, channel preprocessing, and image reconstruction steps were used as in Experiment 1.

Statistical analyses

Behavioral analyses

In the change detection tasks, it was examined how trial type (same, different) and movement (no move, active move) influenced outcome-based and mouse-tracking measures. I used a 2x2 repeated-measures ANOVA to analyze the same behavioral dependent variables as in Experiment 2, which included accuracy, RT, Pashler's K, AUC, and maximum deviation time.

To account for multiple comparisons, the Bonferroni-Holm correction was applied to all pairwise comparisons.

fNIRS group analyses

A repeated-measures ANOVA with factors of trial type (same, different), movement (no move, active move), and hemoglobin (HbO, HbR) was conducted on the reconstructed fNIRS data. Another repeated-measures ANOVA was conducted to examine neural activity in shape change detection trials (action-relevant trials). For this analysis, the factors of movement (no move, active move), and hemoglobin (HbO, HbR) were included. The HbO and HbR activation maps were analyzed using *3dMVM* in AFNI. Residuals for each voxel were created and subjected to AFNI's *3dClustSim* to determine the minimum cluster size necessary to achieve a family-wise error rate of less than .05 and a voxel-wise threshold of less than .05 (Cox et al., 2017).

Behavioral results

Movement encoding accuracy

Movement accuracy in the active move task was 88.25%. Accurate movement responses that occurred during the encoding display (i.e., within 800 ms) was 84.09%. A between-experiment analysis using an independent samples *t*-test showed that movement accuracy during encoding was significantly higher in the active move task in Experiment 3 (M = 84.09%) than the active move task in Experiment 2 (M = 78.52%), $t(62) = 2.42$, $p = .018$. This result suggests that the more complicated design used in Experiment 2 (three alternating tasks) compared to Experiment 3 (two alternating tasks) introduced additional task demands as suspected.

Shape change detection accuracy

Overall shape change detection accuracy was high across the no move and active move tasks (M = 96.6%). Shape change detection accuracy was significantly higher in the active move task (M = 98.67%) compared to the no move task (M = 94.69%), $t(31) = 2.35$, $p = .025$ (Figure 15). This result suggests that VWM for action-relevant features (i.e., the shapes) was enhanced in the active move block (Table 5).

Overall change detection accuracy

The effect of trial type on change detection accuracy was marginally significant, $F(1,31) = 3.564$, $p = .068$, $\eta_p^2 = .103$, with same trials (M = 86.2%) having higher accuracy than different trials (M = 83.8%). There was a significant effect of movement on accuracy, $F(1,31) = 10.34$, $p = .003$, $\eta_p^2 = .250$. No move trials (M = 89.6%) had significantly higher accuracy than active move trials (M = 80.4%), indicating that VWM was worsened for action-irrelevant features (i.e., color) in the active move task. There was no trial type x movement interaction effect, $F = 1.4$. Accuracy results can be seen in Figure 16a.

Pashler's K

VWM capacity as estimated with Pashler's K was significantly higher in the no move (M = 3.16) compared to the active move change detection task (M = 2.42), $t(31) = 3.21$, $p = .003$ (Figure 16b). This result suggests that VWM capacity was worsened when an action-irrelevant response was required in the active move task.

Reaction time

There was a significant effect of trial type on RT, $F(1,31) = 7.36$, $p = .010$, $\eta_p^2 = .204$. Pairwise comparisons showed that RTs were significantly faster on same (M = 1202.78 ms) than

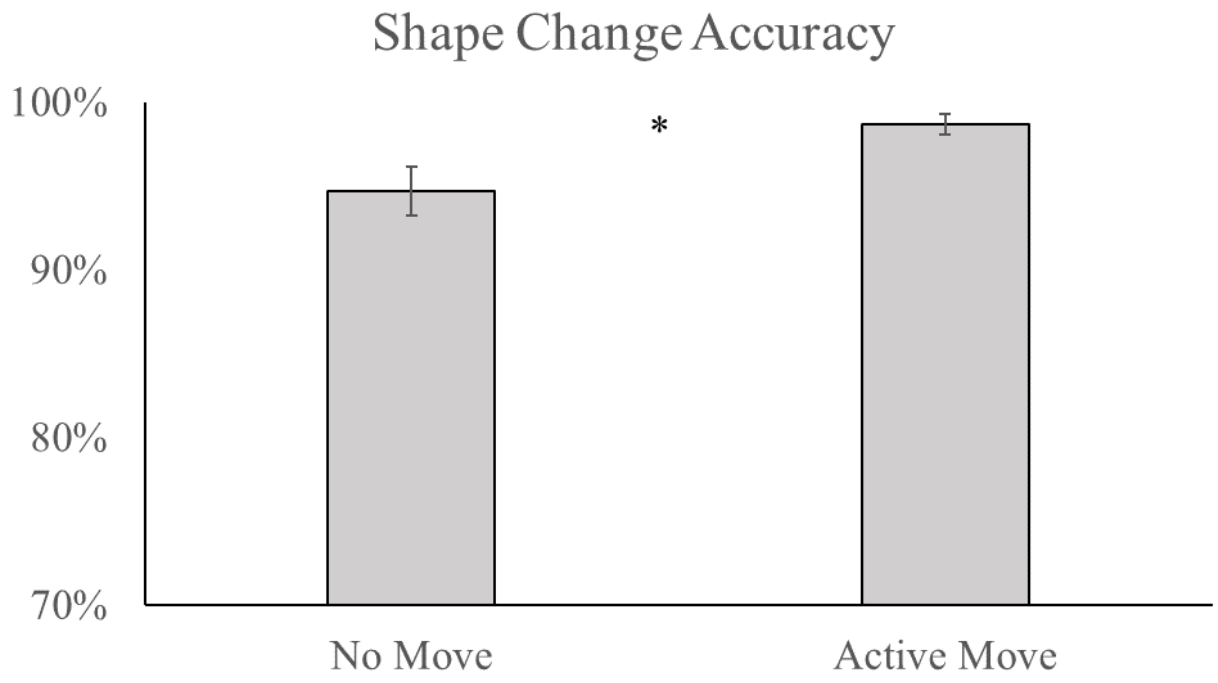

Figure 15. Experiment 3 Shape Change Accuracy Results. * $p < .05$. Error bars display SEM.

Table 5. Action-relevant and action-irrelevant effects on change detection accuracy

Experiment	Change Dimension	Action-relevant	Pairwise Comparison	*t*	Action Enhancement or Inhibition
2	Color	No	Passive move – No move	-1.30	No
	Color	No	Active move – No move	-1.20	No
	Shape	Yes	Passive move – No move	0.21	No
	Shape	Yes	Active move – No move	0.94	No
3	Color	No	Active move – No move	-3.20*	Inhibition
	Shape	Yes	Active move – No move	2.35*	Enhancement

Note. * $p < .05$.

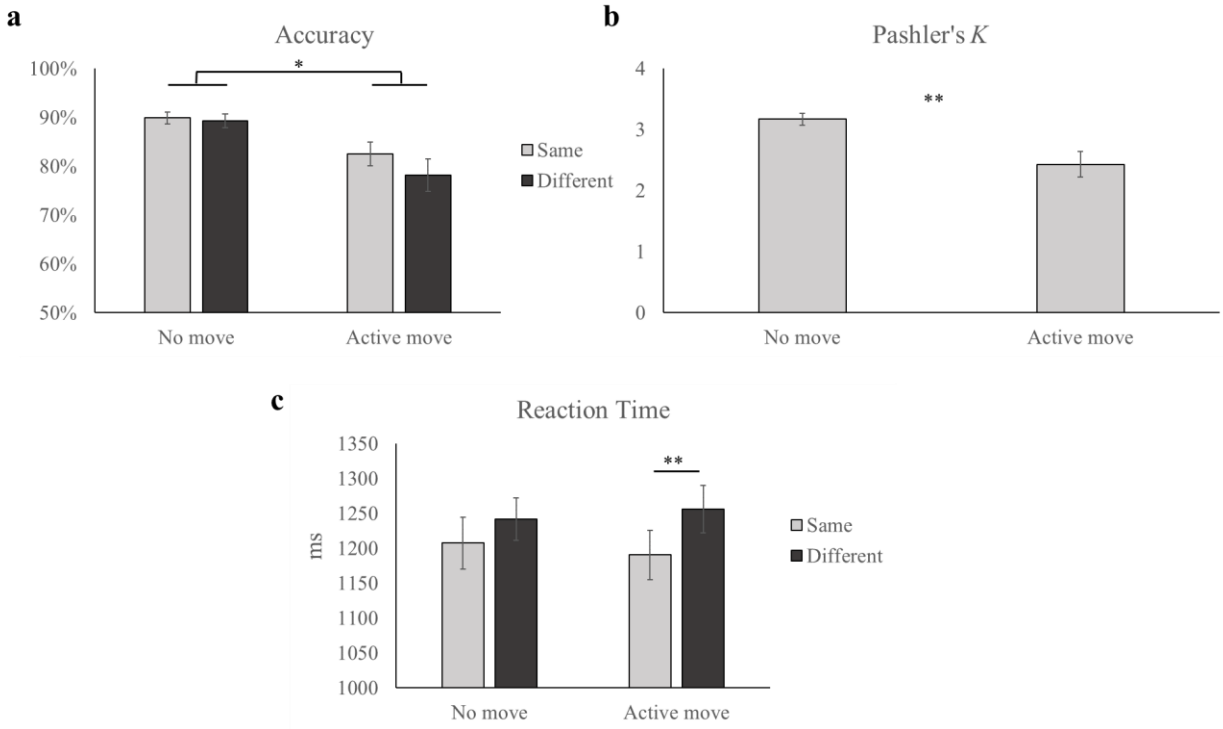

Figure 16. Experiment 3 Outcome-based Results. **a.** Accuracy for each condition. **b.** Pashler's *K* for each movement type. **c.** RT for each condition. Error bars display SEM. * $p < .05$. ** $p < .01$.

different trials (M = 1250.01 ms; Figure 16c). There was no effect of movement on RT, $F < 1$, and there was not a trial type x movement interaction effect, F =2.4.

Area under the curve

There was a significant effect of trial type on AUC, $F(1,31) = 5.36$, p =.028, η_p^2 = .152. Pairwise comparisons showed that AUC was larger on different (M = .585) compared to same trials (M = .404; Figure 17a). There was no significant effect of movement on AUC, F = 2.2, and there was not a significant trial type x movement interaction effect, $F < 1$.

Maximum deviation time

There was a significant effect of trial type on MD time, $F(1,31) = 10.23$, p =.003, η_p^2 = .254. Same trials (M = 614.79 ms) reached MD significantly sooner than different trials (M = 653.85 ms; Figure 17b). There was no effect of movement on MD time, $F < 1$, and there was not a trial type x movement interaction effect, F = 2.6.

fNIRS results

To investigate how action-irrelevance (color dimension test trials) affected VWM performance and neural activity in the change detection task, reconstructed fNIRS data were analyzed with AFNI's *3dMVM* using a repeated-measures ANOVA design with movement (no move, active move), trial type (same, different), and hemoglobin (HbO, HbR) as factors. An additonal ANOVA was conducted to examine the impact of action-relevance (shape dimension change trials) on VWM neural activiation. This ANOVA had two factors: movement (no move, active move) and hemoglobin (HbO, HbR).

Action-irrelevant group effects

Frontal cortex. There was a significant movement x hemoglobin interaction in a cluster in SFG, F (1,30) = 6.45, p = .016, η_p^2 = .177 (Figure 18a). A simple main effect analysis revealed that the interaction was by greater HbO concentration on no move trials (M = .058) compared to active move trials (M = .004), p = .014. However, in the no move condition, HbO was not significantly greater than HbR (M = .004), p = .304.

Posterior parietal cortex. There was a significant move x change x hemoglobin three-way interaction in a cluster in the angular gyrus, F (1,29) = 5.39, p = .027, η_p^2 = .157 (Figure 18b). On active move different trials (M = .118), HbO concentration was significantly greater compared to no move different trials (M = .001), p = .017. However, HbO was not significantly greater than HbR (M = -.008) on active move different trials, p = .189. A summary of the action-irrelevant group effects can be found in Table 6.

Action-relevant group effects

Frontal cortex. There was a cluster in SFG that showed a significant difference between HbO and HbR, t (31) = 2.57, p = .015 (Figure 19a; Table 7), indicating that this region was engaged during shape change detection trials. There was also a movement x hemoglobin interaction effect found in MFG, F (1,30) = 6.39, p = .017, η_p^2 = .176 (Figure 19b). This interaction was driven by HbO (M = .092) being significantly greater than HbR (M = -.092) on no move trials (p = .048), but not on active move trials (p = .202). This result suggests that MFG activity was associated with VWM encoding during no move trials, but not active move trials.

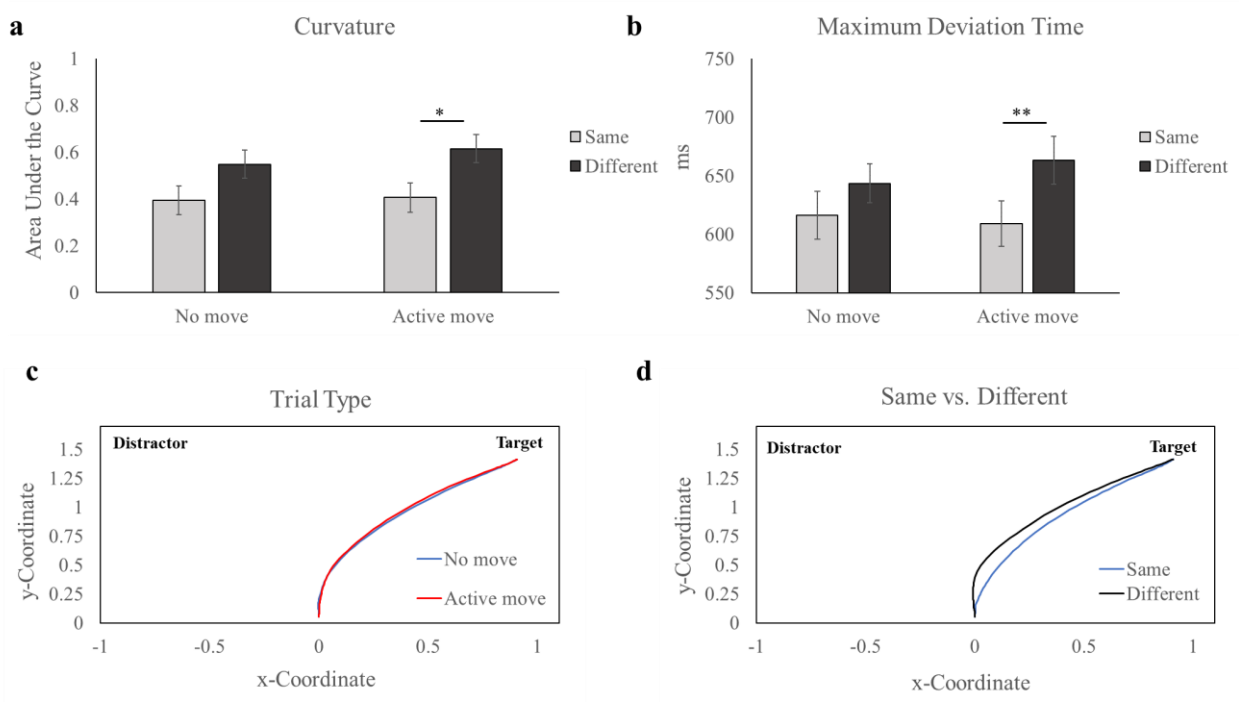

Figure 17. Experiment 3 Mouse-tracking Results. **a.** AUC scores for each condition. **b.** MD Time across conditions. **c.** Mean trajectories plotted for each move type. d. Mean trajectories plotted for each trial type. Error bars display SEM. * $p < .05$. ** $p < .01$.

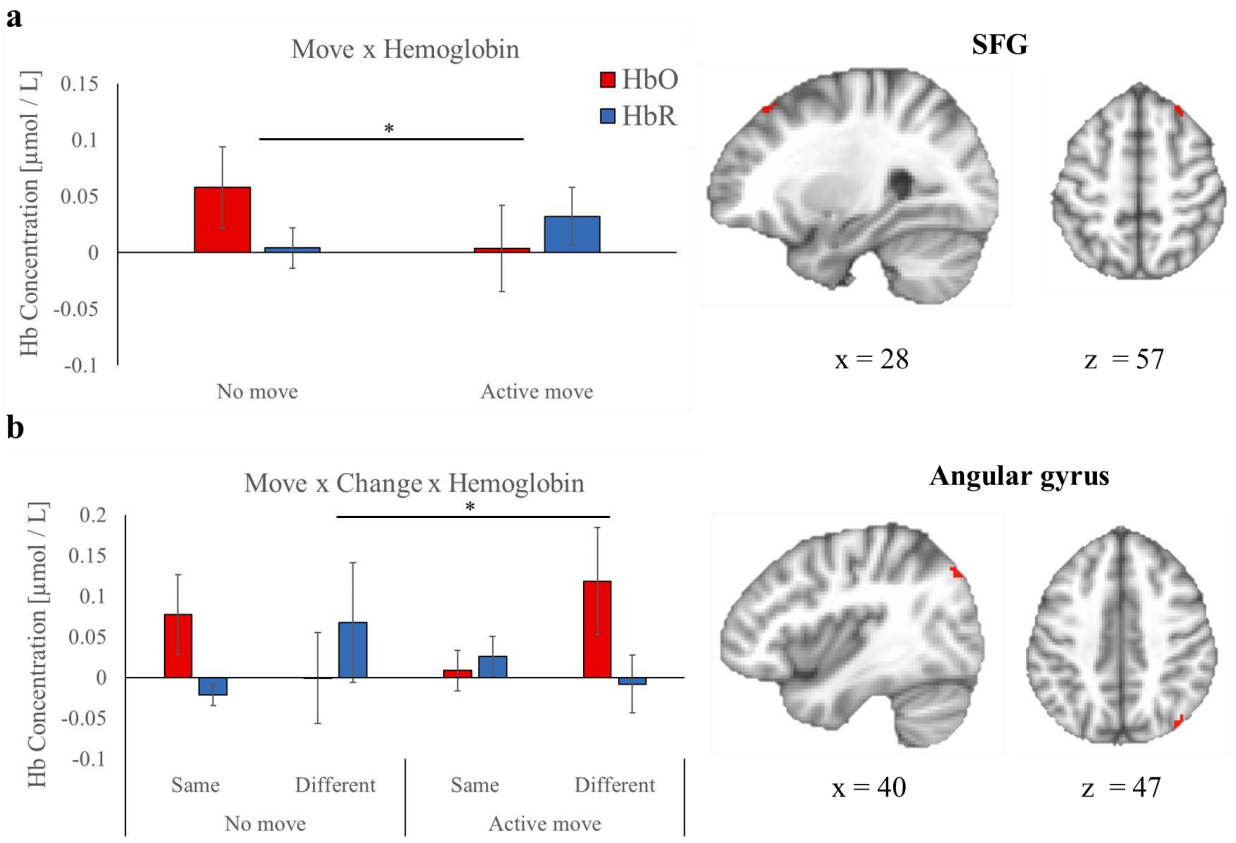

Figure 18. Experiment 3 Action-irrelevant fNIRS Group Effects. **a.** Move x hemoglobin interaction SFG. **b.** Move x change x hemoglobin interaction found in the angular gyrus. Error bars display SEM. * $p < .05$.

Table 6. Summary of fNIRS group effects for action-irrelevant trials in Experiment 3

Effect	Region	Cluster Size (# voxels)	MNI Coordinates (x, y, z)	*F* value
Move x Hemoglobin	SFG	21	28, 30, 57	6.46*
Move x Change x Hemoglobin	Angular gyrus	30	40, -80, 47	5.39*

Note. * $p < .05$.

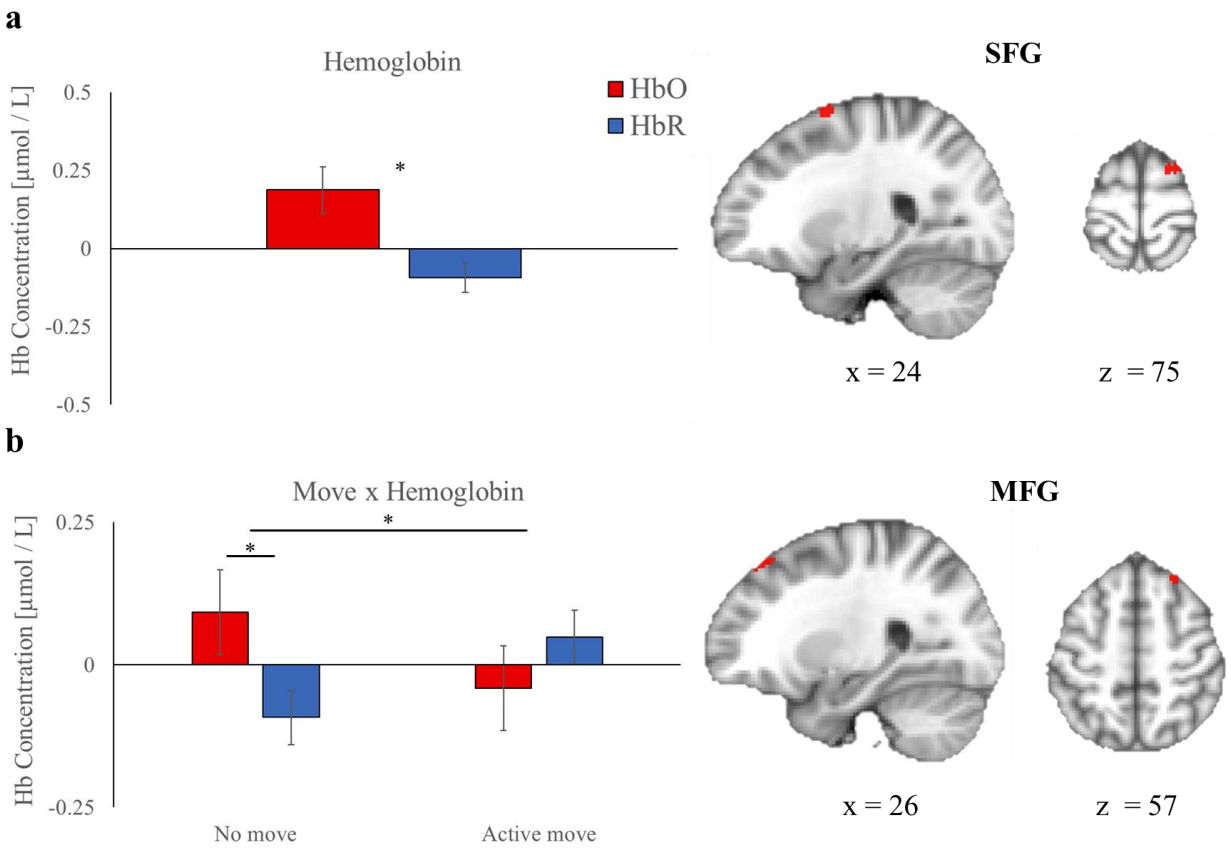

Figure 19. Experiment 3 Action-relevant fNIRS Group Effects. **a.** Hemoglobin main effect in SFG. **b.** Move x hemoglobin interaction in MFG. Error bars display SEM. * $p < .05$.

Table 7. Summary of fNIRS group effects for action-relevant trials in Experiment 3

Effect	Region	Cluster Size (# voxels)	MNI Coordinates (x, y, z)	*F* value
Hemoglobin	SMA	83	24, 2, 75	6.61*
Move x Hemoglobin	SFG	33	26, 30, 57	6.39*

Note. * $p < .05$.

fNIRS and behavioral correlations

Bivariate correlation analyses were conducted in SPSS and AFNI's 3dttest+ function to examine the relationship between neural and mouse-tracking measures, as done in Experiment 1. Voxel-wise residuals from each correlation analysis were used to estimate the minimum cluster size required to achieve significance ($p < 0.05$). The beta weights from the significant correlation clusters were extracted and analyzed to determine the Pearson Correlation Coefficient. To investigate the relationship between memory strength and neural activation, AUC scores were correlated with clusters showing greater HbO than HbR on action-irrelevant and action-relevant trials.

Action-irrelevant correlations

There were no correlations found between no move behavioral performance and neural activity. Below, correlations brain-behavior correlations for active move trials are reported.

Motor cortex. There was a positive correlation between AUC scores and HbO concentration in a cluster in the SMA on active move different trials ($r = .424$, $p = .018$; Figure 20b), indicating that greater activation in this region was associated with worse performance (i.e., more movement curvature).

Posterior parietal cortex. There was a cluster in IPL that showed a negative correlation between AUC and HbO on active move same trials ($r = -.358$, $p = .044$; Figure 20a). Greater activation in IPL was associated with less movement curvature, or better VWM performance. A summary of these correlations can be found in Table 8.

Action-relevant correlations

Frontal cortex. There was a negative correlation between AUC and HbO in SFG on active move trials ($r = -.356$, $p = .046$; Figure 21b).

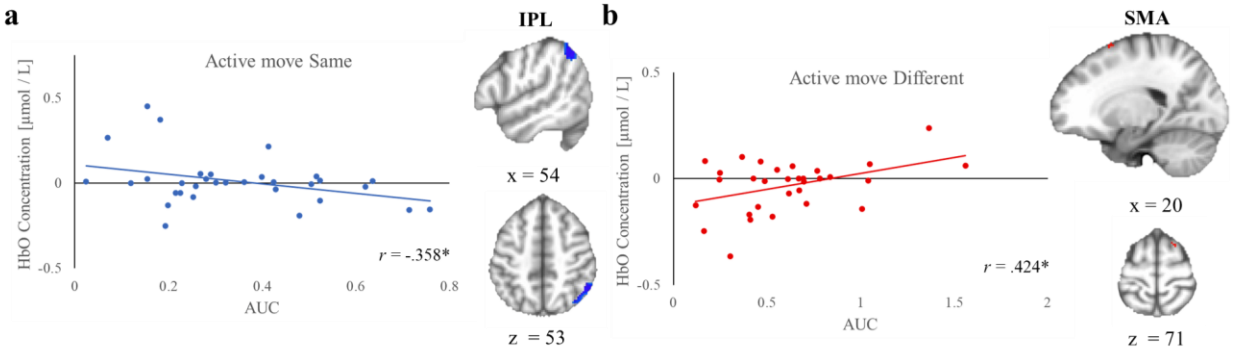

Figure 20. Experiment 3 fNIRS and AUC Correlations for Action-irrelevant Trials.

a. Correlations for move same trials. **b**. Correlations for active move different trials. * $p < .05$.

Table 8. Correlations between AUC and fNIRS data on action-irrelevant trials

Condition	Region	Cluster Size (# voxels)	MNI Coordinates (x, y, z)	*r* value
Active move same	IPL	476	54, -58, 53	-.358*
Active move different	SMA	23	20, 10, 71	.424*

Note. * $p < .05$.

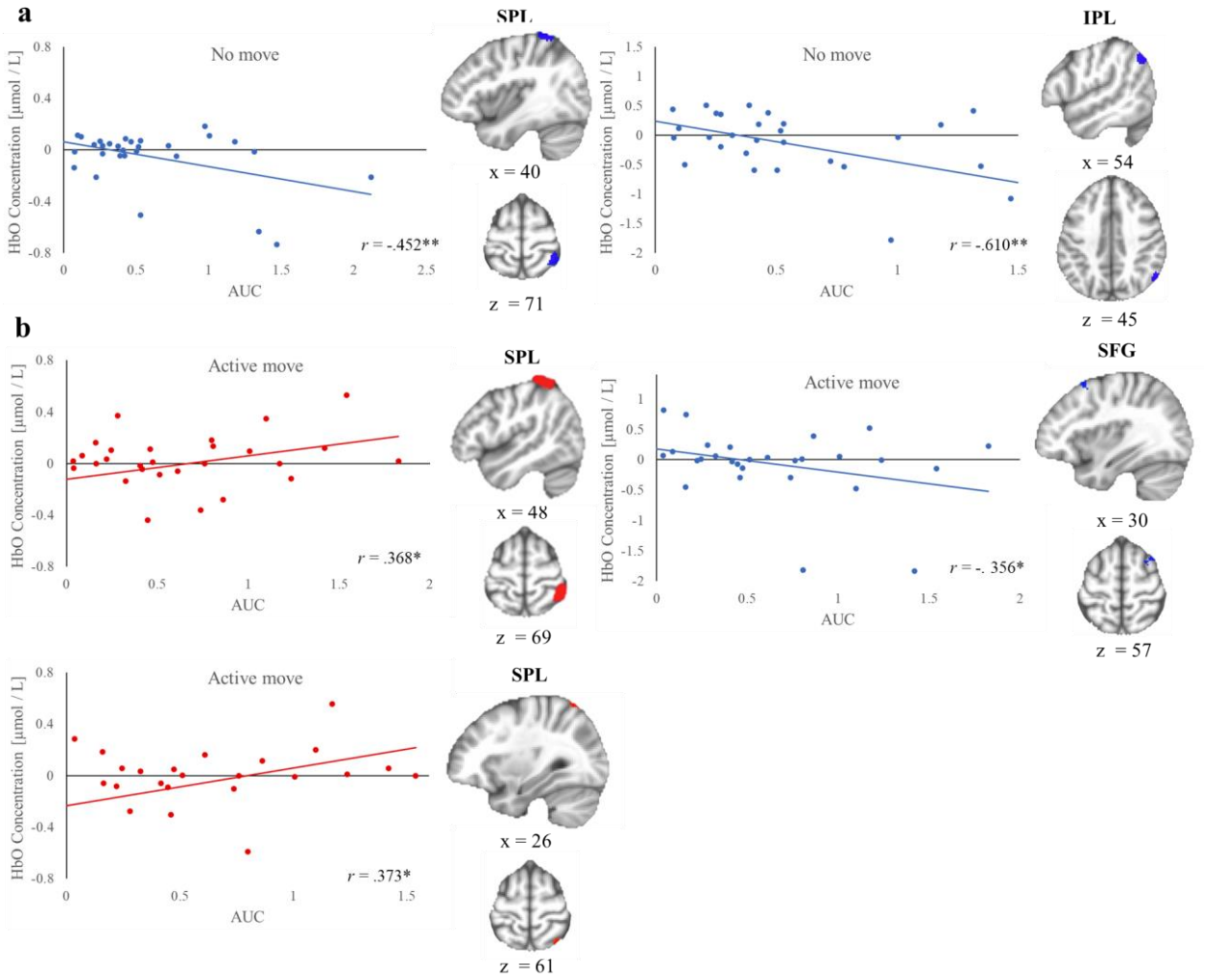

Figure 21. Experiment 3 fNIRS and AUC Correlations for Action-relevant Trials. **a.** Correlations for no move trials. **b.** Correlations for active move trials. * $p < .05$. ** $p < .01$.

Posterior parietal cortex. On no move trials, there were two clusters in posterior parietal cortex that were negatively associated with AUC. First, the HbO concentration in SPL was negatively correlated with AUC (r = -.452, p = .009; Figure 21a). Next, HbO concentration in IPL was strongly negatively correlated with AUC (r = -.610, p < .001; Figure 21a). These results suggest that when no movement was required during VWM encoding, activity in posterior parietal cortex during encoding predicted enhanced VWM performance.

On active move trials, the opposite result was found in posterior parietal cortex compared to no move trials. Two clusters in SPL had HbO concentrations that were found to be positively correlated with AUC scores (r = .368, p = .042 & r = .373, p = .05; Figure 21b). When a movement was required during encoding and the action-relevant dimension was tested, participants with greater activity in posterior parietal cortex predicted worse behavioral performance (i.e., greater AUC scores). A summary of these correlations can be found in Table 9.

Table 9. Correlations between AUC and fNIRS data on action-relevant trials

Condition	Region	Cluster Size (# voxels)	MNI Coordinates (x, y, z)	*r* value
No move	SPL	97	40, -54, 71	-.452**
	IPL	80	54, -64, 45	-.610**
Active move	SPL	290	48, -50, 69	.368*
	SFG	32	30, 28, 57	-.356*
	SPL	21	26, -80, 61	.373*

Note. * $p < .05$. ** $p < .01$.

Chapter 5: General Discussion

VWM is a fundamental aspect of cognition that guides our motor system toward relevant information in the environment. Although it is well-established that VWM and the motor system work closely together to produce goal-directed behavior, there is a gap in our understanding of how action affects VWM encoding and VWM representations. To address this open question the present study investigated the impact of motor responses on VWM encoding using movement dynamics and neural activity measurements during a series of change detection tasks.

The first aim of this thesis was to examine the relationship between movement dynamics, VWM performance, and their associated neural activity in a standard version of the change detection task (Experiment 1). To accomplish this, a novel mouse-tracking and fNIRS change detection task design was employed. The behavioral results of the study supported previous research (Wijeakumar et al., 2017), showing that performance worsened as set size increased (i.e., lower accuracy and slower response times) and that VWM capacity was limited to around 3-4 items (Luck & Vogel, 1997). The mouse-tracking measures revealed similar findings, with response curvature (AUC) increasing as set size increased, and MD time being reached sooner at lower set sizes. Moreover, the study found that response curvature correlated with VWM demands, which expands on previous research linking curvature to long-term memory strength (Papesh & Goldinger, 2012).

Experiment 1 yielded several behavioral results indicating better performance for same compared to different trials. This same response bias is a common finding in the VWM literature and it is known to become stronger as set size increases (e.g., Costello & Buss, 2018). In the whole report version of the change detection task used in the study, participants were required to detect whether a single item had changed among all the presented items. At higher set sizes, this

means there were more same items than different items (e.g., SS4: 3:1 same-different item ratio), leading to input that is more congruent with the same response option. I used movement trajectory analyses to investigate three possible explanations for this same response bias: (1) early "same" activation driving decision evidence towards the same response on same trials, (2) early "same" activation recruiting additional top-down VWM comparison resources on different trials, requiring more time for response selection processes to resolve competition, or (3) a combination of both, leading to enhanced performance on same trials and impaired performance on different trials. For each above explanation, higher set sizes should strengthen each effect due to the increasing number of "same" items. On same trials, I found that the time at which trajectories began to deviate towards the same response was similar across all set sizes. However, on different trials, trajectories deviated towards the different response (i.e., the target location) systematically later in time as set size increased. This suggests that participants may not be biased towards selecting the same response on same trials, even at higher set sizes where more items do not change. Rather, the additional recruitment of VWM comparison processes at higher set sizes my worsen both the ability and time it takes to detect a change when one is present. Specifically, conducting VWM comparison processes on numerous same items may tax the VWM system, worsening representations and increasing uncertainty, making it less likely to reach the activation threshold for detecting a change in the different item. These results make an interesting contribution to the VWM literature and have implications for our present understanding of VWM dynamics in the change detection task. Future implementations of change detection tasks should consider how same and different responses can be influenced based on the set size and type of change detection design (e.g., whole report vs. single report).

In Experiment 1, neural data from the change detection task activated regions commonly associated with the VWM frontoparietal network, including IPL, SPL, MFG, and SFG (Linden et al., 2003; Pessoa & Ungerleider, 2004; Todd & Marois, 2004; Wijeakumar et al., 2017). Specifically, a SFG cluster was found to be engaged in the change detection task collapsed across all conditions, while an IFG cluster was only activated when VWM capacity was near capacity (SS4). Posterior parietal cortex activation varied with set size, but not in a linear manner as expected. While SS4 showed greater activation than SS3 in this region, activity between SS4 and SS2 trials did not vary. In previous research (Todd & Marois, 2004) it has been shown that activation in posterior parietal cortex linearly increases from SS1 to SS4 until plateauing (thought to reflect reaching VWM capacity). It is possible that my finding shows part of posterior parietal cortex being recruited specifically when VWM demands are at or near capacity (SS4). Indeed, the intra parietal sulcus (IPS) reported by Todd and Marois (2004) is located superiorly to the cluster in angular gyrus reported here. The lack of a linear effect of set size on neural activity in this region may be due to a lack of required statistical power. That is, it is possible that there were not enough overlapping fNIRS probe placements over IPS to detect a significant linear effect of set size.

In Experiments 2 & 3, the focus was on examining the impact of action on VWM encoding. To this end, I manipulated task-relevance of the action in Experiment 2 and action-relevance of the dimension of items being encoded in Experiments 2 & 3. Experiment 2 included a task-relevance manipulation to better understand the effect of action on memory encoding. Previous work has shown that task-irrelevant (Shimane et al., 2022) and task-relevant (Kinder & Buss, 2021) items encoded into long-term memory can be improved by motor engagement; however, the link between VWM encoding and actions task-relevance is unclear. Contrary to

expectations, Experiment 2 did not reveal an effect of action on either task-relevant or task-irrelevant items in VWM, compared to a no movement control condition. Further, I did not find the common change detection result (as seen in Experiment 1) that same trials typically have better performance than different trials overall. These results suggest that VWM processes may have been taxed by the high demands of randomly switching between three different tasks (no move, passive move, and the active move change detection tasks). Another result supporting this interpretation is that movement accuracy during encoding in the passive and active move blocks were much lower than expected. Experiment 3 used a simplified design (no move and active move; two alternating tasks), and with this I found (1) better performance on same compared to different trials as expected, and (2) higher movement encoding accuracy for the active move change detection task used in Experiment 3 compared to the one used in Experiment 2. Overall, these results indicate that the complex design used in Experiment 2 likely imposed high task demands that negatively affected change detection performance and disrupted motor engagement processes in the passive and active move change detection tasks.

Experiment 3 provided a behavioral and neural dataset that combined mouse-tracking and fNIRS to investigate the effect of action on VWM encoding. This experiment manipulated whether an action was required during VWM encoding and whether the features of the items tested were action-relevant or action-irrelevant. Behavioral results revealed that performance, including accuracy and Pashler's *K*, was better for no move compared to when action-irrelevant (i.e., color) features were tested. However, when action-relevant features (i.e., shape) were tested, the opposite pattern of results was found, with there being higher accuracy compared to the no move change detection task. This set of results suggests that action improved the VWM encoding of features that were relevant to the action, but inhibited the encoding of features that

were irrelevant to the action. These results build upon other studies that manipulated whether the action was directed towards an action-relevant or -irrelevant spatial location during maintenance (Heuer et al., 2017; Heuer et al., 2020), and suggest that both the enhancement of action-relevant features and the inhibition of action-irrelevant features during VWM encoding. The fNIRS results showed that activation in frontal cortex was linked to enhanced VWM encoding for action-relevant features. On the other hand, activation in posterior parietal cortex was associated with enhanced VWM encoding for action-irrelevant features and those that were unrelated to action (no move). Interestingly, for action-relevant items, greater activation in posterior parietal cortex was detrimental to VWM performance. These findings suggest that the VWM network is differentially activated when encoding features that are action-relevant or action-irrelevant.

The findings of this thesis are consistent with theories of embodied cognition. From this perspective, the motor system holds a significant role in cognition, rather than simply serving as its output. That is, cognition is proposed to be grounded and emerges from environmental interactions tied to sensorimotor systems (Chiel & Beer, 1997), and emphasizes a bidirectional relationship in which both the motor and cognitive systems can continuously exchange information (Thelen & Smith, 1996). This view regards the motor system as a fundamental aspect of cognition. This thesis expands on embodied cognition perspectives by showing that the influence of action on VWM encoding depends on action-relevance.

Chapter 6: Conclusion

This thesis presented an account of action's effect on memory encoding that was examined in the context of a VWM change detection task. The results of this work provide new insights into VWM processes in the change detection task and have theoretical implications for the relationship between action and memory. Results showed that the strength of VWM memory representations can be measured with a mouse-tracking method that is sensitive to temporal dynamics, which can be used to better understand VWM effects such as the same response bias examined here. My main results demonstrated that action enhances VWM encoding for action-relevant features but impairs memory for action-irrelevant features. This suggests that the motor system may allocate VWM resources toward action-relevant features, while diverting VWM resources away from action-irrelevant features. In other words, the motor system may differentially impact the representations of features held in VWM depending on their action-relevance. Furthermore, the fNIRS data indicated that activation in frontal cortex is related to enhanced VWM encoding for action-relevant items. Alternatively, it was found that activation in posterior parietal cortex was associated with enhanced VWM encoding for action-irrelevant items and when no movement was required. Interestingly, for action-relevant items, increased activation in posterior parietal cortex resulted in impaired memory performance. These results provide new insights into the neural dynamics involved in VWM encoding and demonstrate how the frontoparietal VWM network may be differentially activated depending on the action-relevance of the encoded. Future research that combines continuous behavioral and neural measures is positioned to provide a more comprehensive understanding of the relationship between memory and action.

References

Aagten-Murphy, D., & Bays, P. M. (2019). Independent working memory resources for egocentric and allocentric spatial information. *PLOS Computational Biology*, *15*(2), e1006563. https://doi.org/10.1371/journal.pcbi.1006563

Aasted, C. M., Yücel, M. A., Cooper, R. J., Dubb, J., Tsuzuki, D., Becerra, L., Petkov, M. P., Borsook, D., Dan, I., & Boas, D. A. (2015). Anatomical guidance for functional near-infrared spectroscopy: AtlasViewer tutorial. *Neurophotonics*, *2*(2), 020801. https://doi.org/10.1117/1.NPh.2.2.020801

Alloway, T. P., Gathercole, S. E., Kirkwood, H., & Elliott, J. (2009). The Cognitive and Behavioral Characteristics of Children With Low Working Memory: Cognitive and Behavioral Characteristics of Low Working Memory Children. *Child Development*, *80*(2), 606–621. https://doi.org/10.1111/j.1467-8624.2009.01282.x

Allport, A. (Ed.). (2016). Selection for Action: Some Behavioral and Neurophysiological Considerations of Attention and Action. In *Perspectives on Perception and Action* (1st ed., pp. 409–434). Routledge. https://doi.org/10.4324/978131562799-25

Andersen, R. A., & Buneo, C. A. (2002). Intentional Maps in Posterior Parietal Cortex. *Annual Review of Neuroscience*, *25*(1), 189–220. https://doi.org/10.1146/annurev.neuro.25.112701.142922

Andersen, R. A., & Cui, H. (2009). Intention, Action Planning, and Decision Making in Parietal-Frontal Circuits. *Neuron*, *63*(5), 568–583. https://doi.org/10.1016/j.neuron.2009.08.028

Baddeley, A. (1992). Working Memory. *Science*, *255*(5044), 556–559. https://doi.org/10.1126/science.1736359

Baddeley, A. (2003). Working memory: Looking back and looking forward. *Nature Reviews Neuroscience*, *4*(10), 829–839. https://doi.org/10.1038/nrn1201

Baldauf, D., Wolf, M., & Deubel, H. (2006). Deployment of visual attention before sequences of goal-directed hand movements. *Vision Research*, *46*(26), 4355–4374. https://doi.org/10.1016/j.visres.2006.08.021

Ballard, D. H., Hayhoe, M. M., Pook, P. K., & Rao, R. P. N. (1997). Deictic codes for the embodiment of cognition. *Behavioral and Brain Sciences*, *20*(4), 723–742. https://doi.org/10.1017/S0140525X97001611

Baty, F., & Delignette-Muller, M.-L. (2004). Estimating the bacterial lag time: Which model, which precision? *International Journal of Food Microbiology*, *91*(3), 261–277. https://doi.org/10.1016/j.ijfoodmicro.2003.07.002

Belopolsky, A. V., & Theeuwes, J. (2011). Selection within visual memory representations activates the oculomotor system. *Neuropsychologia*, *49*(6), 1605–1610. https://doi.org/10.1016/j.neuropsychologia.2010.12.045

Boon, P. J., Theeuwes, J., & Belopolsky, A. V. (2014). Updating visual–spatial working memory during object movement. *Vision Research*, *94*, 51–57. https://doi.org/10.1016/j.visres.2013.11.002

Borglin, S., Joyner, D., DeAngelis, K. M., Khudyakov, J., D'haeseleer, P., Joachimiak, M. P., & Hazen, T. (2012). Application of phenotypic microarrays to environmental microbiology. *Current Opinion in Biotechnology*, *23*(1), 41–48. https://doi.org/10.1016/j.copbio.2011.12.006

Bosco, A., Daniele, F., & Fattori, P. (2017). Reaching and grasping actions and their context shape the perception of object size. *Journal of Vision*, *17*(12), 10. https://doi.org/10.1167/17.12.10

Brady, T. F., Konkle, T., & Alvarez, G. A. (2011). A review of visual memory capacity: Beyond individual items and toward structured representations. *Journal of Vision*, *11*(5), 4–4. https://doi.org/10.1167/11.5.4

Campbell, J. I. D., & Thompson, V. A. (2012). MorePower 6.0 for ANOVA with relational confidence intervals and Bayesian analysis. *Behavior Research Methods*, *44*(4), 1255–1265. https://doi.org/10.3758/s13428-012-0186-0

Chen, G., Adleman, N. E., Saad, Z. S., Leibenluft, E., & Cox, R. W. (2014). Applications of multivariate modeling to neuroimaging group analysis: A comprehensive alternative to univariate general linear model. *NeuroImage*, *99*, 571–588. https://doi.org/10.1016/j.neuroimage.2014.06.027

Chiel, H. J., & Beer, R. D. (1997). The brain has a body: Adaptive behavior emerges from interactions of nervous system, body and environment. *Trends in Neurosciences*, *20*(12), 553–557. https://doi.org/10.1016/S0166-2236(97)01149-1

Clark, J. H. (1924). The Ishihara Test for Color Blindness. *American Journal of Physiological Optics*, *5*, 269–276.

Cisek, P., & Kalaska, J. F. (2005). Neural Correlates of Reaching Decisions in Dorsal Premotor Cortex: Specification of Multiple Direction Choices and Final Selection of Action. *Neuron*, *45*(5), 801–814. https://doi.org/10.1016/j.neuron.2005.01.027

Costello, M. C., & Buss, A. T. (2018). Age-related Decline of Visual Working Memory: Behavioral Results Simulated with a Dynamic Neural Field Model. *Journal of Cognitive Neuroscience*, *30*(10), 1532–1548. https://doi.org/10.1162/jocn_a_01293

Cowan, N. (2001). The magical number 4 in short-term memory: A reconsideration of mental storage capacity. *Behavioral and Brain Sciences*, *24*(1), 87–114. https://doi.org/10.1017/S0140525X01003922

Cowan, N., Elliott, E. M., Scott Saults, J., Morey, C. C., Mattox, S., Hismjatullina, A., & Conway, A. R. A. (2005). On the capacity of attention: Its estimation and its role in working memory and cognitive aptitudes. *Cognitive Psychology*, *51*(1), 42–100. https://doi.org/10.1016/j.cogpsych.2004.12.001

Cox, R. W., Chen, G., Glen, D. R., Reynolds, R. C., & Taylor, P. A. (2017). FMRI Clustering in AFNI: False-Positive Rates Redux. *Brain Connectivity*, *7*(3), 152–171. https://doi.org/10.1089/brain.2016.0475

Dai, M., Li, Y., Gan, S., & Du, F. (2019). The reliability of estimating visual working memory capacity. *Scientific Reports*, *9*(1), 1155. https://doi.org/10.1038/s41598-019-39044-1

Defenderfer, J., Forbes, S., Wijeakumar, S., Hedrick, M., Plyler, P., & Buss, A. T. (2021). Frontotemporal activation differs between perception of simulated cochlear implant speech and speech in background noise: An image-based fNIRS study. *NeuroImage*, *240*, 118385. https://doi.org/10.1016/j.neuroimage.2021.118385

Delpy, D. T., Cope, M., Zee, P. van der, Arridge, S., Wray, S., & Wyatt, J. (1988). Estimation of optical pathlength through tissue from direct time of flight measurement. *Physics in Medicine and Biology*, *33*(12), 1433–1442. https://doi.org/10.1088/0031-9155/33/12/008

Doyle, M., & Walker, R. (2001). Curved saccade trajectories: Voluntary and reflexive saccades curve away from irrelevant distractors. *Experimental Brain Research*, *139*(3), 333–344. https://doi.org/10.1007/s002210100742

Eggebrecht, A. T., Ferradal, S. L., Robichaux-Viehoever, A., Hassanpour, M. S., Dehghani, H., Snyder, A. Z., Hershey, T., & Culver, J. P. (2014). Mapping distributed brain function and networks with diffuse optical tomography. *Nature Photonics*, *8*(6), 448–454. https://doi.org/10.1038/nphoton.2014.107

Fang, Q., & Boas, D. A. (2009). Monte Carlo Simulation of Photon Migration in 3D Turbid Media Accelerated by Graphics Processing Units. *Optics Express*, *17*(22), 20178. https://doi.org/10.1364/OE.17.020178

Forbes, S. H., Wijeakumar, S., Eggebrecht, A. T., Magnotta, V. A., & Spencer, J. P. (2021). *A processing pipeline for image reconstructed fNIRS analysis using both MRI templates and individual anatomy* [Preprint]. Neuroscience. https://doi.org/10.1101/2021.01.14.426719

Freeman, J. B., & Ambady, N. (2009). Motions of the Hand Expose the Partial and Parallel Activation of Stereotypes. *Psychological Science*, *20*(10), 1183–1188. https://doi.org/10.1111/j.1467-9280.2009.02422.x

Freeman, J. B., & Ambady, N. (2010). MouseTracker: Software for studying real-time mental processing using a computer mouse-tracking method. *Behavior Research Methods*, *42*(1), 226–241. https://doi.org/10.3758/BRM.42.1.226

Fukuda, K., Vogel, E., Mayr, U., & Awh, E. (2010). Quantity, not quality: The relationship between fluid intelligence and working memory capacity. *Psychonomic Bulletin & Review*, *17*(5), 673–679. https://doi.org/10.3758/17.5.673

Goodwin, J. R., Gaudet, C. R., & Berger, A. J. (2014). Short-channel functional near-infrared spectroscopy regressions improve when source-detector separation is reduced. *Neurophotonics*, *1*(1), 015002. https://doi.org/10.1117/1.NPh.1.1.015002

Grèzes, J., Tucker, M., Armony, J., Ellis, R., & Passingham, R. E. (2003). Objects automatically potentiate action: An fMRI study of implicit processing: Implicit processing of affordances. *European Journal of Neuroscience*, *17*(12), 2735–2740. https://doi.org/10.1046/j.1460-9568.2003.02695.x

Gulbinaite, R., & Johnson, A. (2014). Working Memory Capacity Predicts Conflict-Task Performance. *Quarterly Journal of Experimental Psychology*, *67*(7), 1383–1400. https://doi.org/10.1080/17470218.2013.863374

Gutteling, T. P., Kenemans, J. L., & Neggers, S. F. W. (2011). Grasping Preparation Enhances Orientation Change Detection. *PLoS ONE*, *6*(3), e17675. https://doi.org/10.1371/journal.pone.0017675

Gutteling, T. P., Petridou, N., Dumoulin, S. O., Harvey, B. M., Aarnoutse, E. J., Kenemans, J. L., & Neggers, S. F. W. (2015). Action Preparation Shapes Processing in Early Visual Cortex. *Journal of Neuroscience*, *35*(16), 6472–6480. https://doi.org/10.1523/JNEUROSCI.1358-14.2015

Han, S. W., & Kim, M.-S. (2009). Do the contents of working memory capture attention? Yes, but cognitive control matters. *Journal of Experimental Psychology: Human Perception and Performance*, *35*(5), 1292–1302. https://doi.org/10.1037/a0016452

Hanning, N. M., & Deubel, H. (2018). Independent Effects of Eye and Hand Movements on Visual Working Memory. *Frontiers in Systems Neuroscience*, *12*, 37. https://doi.org/10.3389/fnsys.2018.00037

Hanning, N. M., Jonikaitis, D., Deubel, H., & Szinte, M. (2016). Oculomotor selection underlies feature retention in visual working memory. *Journal of Neurophysiology*, *115*(2), 1071–1076. https://doi.org/10.1152/jn.00927.2015

Hehman, E., Stolier, R. M., & Freeman, J. B. (2015). Advanced mouse-tracking analytic techniques for enhancing psychological science. *Group Processes & Intergroup Relations*, *18*(3), 384–401. https://doi.org/10.1177/1368430214538325

Heuer, A., Crawford, J. D., & Schubö, A. (2017). Action relevance induces an attentional weighting of representations in visual working memory. *Memory & Cognition*, *45*(3), 413–427. https://doi.org/10.3758/s13421-016-0670-3

Heuer, A., Ohl, S., & Rolfs, M. (2020). Memory for action: A functional view of selection in visual working memory. *Visual Cognition*, *28*(5–8), 388–400. https://doi.org/10.1080/13506285.2020.1764156

Hoffman, J. E., & Subramaniam, B. (1995). The role of visual attention in saccadic eye movements. *Perception & Psychophysics*, *57*(6), 787–795. https://doi.org/10.3758/BF03206794

Hollingworth, A., & Luck, S. J. (2009). The role of visual working memory (VWM) in the control of gaze during visual search. *Attention, Perception, & Psychophysics*, *71*(4), 936–949. https://doi.org/10.3758/APP.71.4.936

Hübner, R., & Töbel, L. (2012). Does Attentional Selectivity in the Flanker Task Improve Discretely or Gradually? *Frontiers in Psychology*, *3*. https://doi.org/10.3389/fpsyg.2012.00434

Huppert, T. J., Diamond, S. G., Franceschini, M. A., & Boas, D. A. (2009). HomER: A review of time-series analysis methods for near-infrared spectroscopy of the brain. *Applied Optics*, *48*(10), D280. https://doi.org/10.1364/AO.48.00D280

Ikkai, A., & Curtis, C. E. (2011). Common neural mechanisms supporting spatial working memory, attention and motor intention. *Neuropsychologia*, *49*(6), 1428–1434. https://doi.org/10.1016/j.neuropsychologia.2010.12.020

Jonikaitis, D., & Moore, T. (2019). The interdependence of attention, working memory and gaze control: Behavior and neural circuitry. *Current Opinion in Psychology*, *29*, 126–134. https://doi.org/10.1016/j.copsyc.2019.01.012

Kinder, K. T., & Buss, A. T. (2021). The effect of motor engagement on memory: Testing a motor-induced encoding account. *Memory & Cognition*, *49*(3), 586–599. https://doi.org/10.3758/s13421-020-01113-6

Kinder, K. T., Buss, A. T., & Tas, A. C. (2022). Tracking flanker task dynamics: Evidence for continuous attentional selectivity. *Journal of Experimental Psychology: Human Perception and Performance*, *48*(7), 771–781. https://doi.org/10.1037/xhp0001023

Kinder, K. T., Heim, H. L. R., Parker, J., Lowery, K., McCraw, A., Eddings, R. N., Defenderfer, J., Sullivan, J., & Buss, A. T. (2022). Systematic review of fNIRS studies reveals inconsistent chromophore data reporting practices. *Neurophotonics*, *9*(04). https://doi.org/10.1117/1.NPh.9.4.040601

Kolodny, T., Mevorach, C., & Shalev, L. (2017). Isolating response inhibition in the brain: Parietal versus frontal contribution. *Cortex*, *88*, 173–185. https://doi.org/10.1016/j.cortex.2016.12.012

Li, C.-H., He, X., Wang, Y.-J., Hu, Z., & Guo, C.-Y. (2017). Visual Working Memory Capacity Can Be Increased by Training on Distractor Filtering Efficiency. *Frontiers in Psychology*, *8*. https://doi.org/10.3389/fpsyg.2017.00196

Linden, D. E. J., Bittner, R. A., Muckli, L., Waltz, J. A., Kriegeskorte, N., Goebel, R., Singer, W., & Munk, M. H. J. (2003). Cortical capacity constraints for visual working memory: Dissociation of fMRI load effects in a fronto-parietal network. *NeuroImage*, *20*(3), 1518–1530. https://doi.org/10.1016/j.neuroimage.2003.07.021

Luck, S. J., & Vogel, E. K. (1997). The capacity of visual working memory for features and conjunctions. *Nature*, *390*(6657), 279–281. https://doi.org/10.1038/36846

Luck, S. J., & Vogel, E. K. (2013). Visual working memory capacity: From psychophysics and neurobiology to individual differences. *Trends in Cognitive Sciences*, *17*(8), 391–400. https://doi.org/10.1016/j.tics.2013.06.006

Luria, R., Balaban, H., Awh, E., & Vogel, E. K. (2016). The contralateral delay activity as a neural measure of visual working memory. *Neuroscience & Biobehavioral Reviews*, *62*, 100–108. https://doi.org/10.1016/j.neubiorev.2016.01.003

March, D. S., & Gaertner, L. (2021). A method for estimating the time of initiating correct categorization in mouse-tracking. *Behavior Research Methods*, *53*(6), 2439–2449. https://doi.org/10.3758/s13428-021-01575-9

Melcher, D., & Piazza, M. (2011). The Role of Attentional Priority and Saliency in Determining Capacity Limits in Enumeration and Visual Working Memory. *PLoS ONE*, *6*(12), e29296. https://doi.org/10.1371/journal.pone.0029296

Milford, M. (n.d.). *TechEn CW7 system*. TechEn Inc.

Molavi, B., & Dumont, G. A. (2012). Wavelet-based motion artifact removal for functional near-infrared spectroscopy. *Physiological Measurement*, *33*(2), 259–270. https://doi.org/10.1088/0967-3334/33/2/259

Monaco, S., Chen, Y., Menghi, N., & Crawford, J. D. (2018). *Action-specific feature processing in the human visual cortex*. Neuroscience. https://doi.org/10.1101/420760

Natick, M. (2022). *MATLAB* (Version 2022a). The MathWorks Inc.

Ohl, S., & Rolfs, M. (2017). Saccadic eye movements impose a natural bottleneck on visual short-term memory. *Journal of Experimental Psychology: Learning, Memory, and Cognition*, *43*(5), 736–748. https://doi.org/10.1037/xlm0000338

Ohl, S., & Rolfs, M. (2018). Saccadic selection of stabilized items in visuospatial working memory. *Consciousness and Cognition*, *64*, 32–44. https://doi.org/10.1016/j.concog.2018.06.016

Ohl, S., & Rolfs, M. (2020). Bold moves: Inevitable saccadic selection in visual short-term memory. *Journal of Vision*, *20*(2), 11. https://doi.org/10.1167/jov.20.2.11

Olivers, C. N. L. (2009). What drives memory-driven attentional capture? The effects of memory type, display type, and search type. *Journal of Experimental Psychology: Human Perception and Performance*, *35*(5), 1275–1291. https://doi.org/10.1037/a0013896

Olivers, C. N. L., Meijer, F., & Theeuwes, J. (2006). Feature-based memory-driven attentional capture: Visual working memory content affects visual attention. *Journal of Experimental Psychology: Human Perception and Performance*, *32*(5), 1243–1265. https://doi.org/10.1037/0096-1523.32.5.1243

Olivers, C. N. L., Peters, J., Houtkamp, R., & Roelfsema, P. R. (2011). Different states in visual working memory: When it guides attention and when it does not. *Trends in Cognitive Sciences*, S1364661311000854. https://doi.org/10.1016/j.tics.2011.05.004

Papesh, M. H., & Goldinger, S. D. (2012). Memory in motion: Movement dynamics reveal memory strength. *Psychonomic Bulletin & Review*, *19*(5), 906–913. https://doi.org/10.3758/s13423-012-0281-3

Pashler, H. (1988). Familiarity and visual change detection. *Perception & Psychophysics*, *44*(4), 369–378. https://doi.org/10.3758/BF03210419

Pasternak, T., & Greenlee, M. W. (2005). Working memory in primate sensory systems. *Nature Reviews Neuroscience*, *6*(2), 97–107. https://doi.org/10.1038/nrn1603

Pessoa, L. (2004). Neural Correlates of Change Detection and Change Blindness in a Working Memory Task. *Cerebral Cortex*, *14*(5), 511–520. https://doi.org/10.1093/cercor/bhh013

Poole-Wilson, P. A., & Langer, G. A. (1975). Effect of pH on ionic exchange and function in rat and rabbit myocardium. *The American Journal of Physiology*, *229*(3), 570–581. https://doi.org/10.1152/ajplegacy.1975.229.3.570

Prinz, W., Beisert, M., & Herwig, A. (Eds.). (2013). *Action Science: Foundations of an Emerging Discipline*. The MIT Press. https://doi.org/10.7551/mitpress/9780262018555.001.0001

Quian Quiroga, R. (2006). Movement Intention Is Better Predicted than Attention in the Posterior Parietal Cortex. *Journal of Neuroscience*, *26*(13), 3615–3620. https://doi.org/10.1523/JNEUROSCI.3468-05.2006

Riley, M. R., & Constantinidis, C. (2016). Role of Prefrontal Persistent Activity in Working Memory. *Frontiers in Systems Neuroscience*, *9*. https://doi.org/10.3389/fnsys.2015.00181

Rouder, J. N., Morey, R. D., Morey, C. C., & Cowan, N. (2011). How to measure working memory capacity in the change detection paradigm. *Psychonomic Bulletin & Review*, *18*(2), 324–330. https://doi.org/10.3758/s13423-011-0055-3

SAS (9.4). (2020). SAS institute.

Savitzky, Abraham., & Golay, M. J. E. (1964). Smoothing and Differentiation of Data by Simplified Least Squares Procedures. *Analytical Chemistry*, *36*(8), 1627–1639. https://doi.org/10.1021/ac60214a047

Schneider, W. X., & Deubel, H. (1995). Visual Attention and Saccadic Eye Movements: Evidence for Obligatory and Selective Spatial Coupling. In *Studies in Visual Information Processing* (Vol. 6, pp. 317–324). Elsevier. https://doi.org/10.1016/S0926-907X(05)80027-3

Shimane, D., Tanaka, T., Watanabe, K., & Tanaka, K. (2022). Motor engagement enhances incidental memory for task-irrelevant items. *Frontiers in Psychology*, *13*, 914877. https://doi.org/10.3389/fpsyg.2022.914877

Singhal, A., Monaco, S., Kaufman, L. D., & Culham, J. C. (2013). Human fMRI Reveals That Delayed Action Re-Recruits Visual Perception. *PLoS ONE*, *8*(9), e73629. https://doi.org/10.1371/journal.pone.0073629

Soto, D., Humphreys, G. W., & Heinke, D. (2006). Working memory can guide pop-out search. *Vision Research*, *46*(6–7), 1010–1018. https://doi.org/10.1016/j.visres.2005.09.008

Spivey, M. J., Grosjean, M., & Knoblich, G. (2005). Continuous attraction toward phonological competitors. *Proceedings of the National Academy of Sciences*, *102*(29), 10393–10398. https://doi.org/10.1073/pnas.0503903102

SPSS (Version 27). (2020). IBM.

Sternberg, S. (1969). The discovery of processing stages: Extensions of Donders' method. *Acta Psychologica*, *30*, 276–315. https://doi.org/10.1016/0001-6918(69)90055-9

Strange, B. A., & Dolan, R. J. (2004). β-Adrenergic modulation of emotional memory-evoked human amygdala and hippocampal responses. *Proceedings of the National Academy of Sciences*, *101*(31), 11454–11458. https://doi.org/10.1073/pnas.0404282101

Tas, A. C., Luck, S. J., & Hollingworth, A. (2016). The relationship between visual attention and visual working memory encoding: A dissociation between covert and overt orienting. *Journal of Experimental Psychology: Human Perception and Performance*, *42*(8), 1121–1138. https://doi.org/10.1037/xhp0000212

Theeuwes, J., Olivers, C. N. L., & Chizk, C. L. (2005). Remembering a Location Makes the Eyes Curve Away. *Psychological Science*, *16*(3), 196–199. https://doi.org/10.1111/j.0956-7976.2005.00803.x

Thelen, E., & Smith, L. B. (1996). *A dynamic systems approach to the development of cognition and action*. MIT press.

Tillman, C. M., Nyberg, L., & Bohlin, G. (2008). Working memory components and intelligence in children. *Intelligence*, *36*(5), 394–402. https://doi.org/10.1016/j.intell.2007.10.001

Todd, J. J., & Marois, R. (2004). Capacity limit of visual short-term memory in human posterior parietal cortex. *Nature*, *428*(6984), 751–754. https://doi.org/10.1038/nature02466

Todd, J. J., & Marois, R. (2005). Posterior parietal cortex activity predicts individual differences in visual short-term memory capacity. *Cognitive, Affective, & Behavioral Neuroscience*, *5*(2), 144–155. https://doi.org/10.3758/CABN.5.2.144

Unsworth, N., Fukuda, K., Awh, E., & Vogel, E. K. (2015). Working Memory Delay Activity Predicts Individual Differences in Cognitive Abilities. *Journal of Cognitive Neuroscience*, *27*(5), 853–865. https://doi.org/10.1162/jocn_a_00765

Unsworth, N., Redick, T. S., Spillers, G. J., & Brewer, G. A. (2012). Variation in working memory capacity and cognitive control: Goal maintenance and microadjustments of control. *Quarterly Journal of Experimental Psychology*, *65*(2), 326–355. https://doi.org/10.1080/17470218.2011.597865

Vossel, S., Geng, J. J., & Fink, G. R. (2014). Dorsal and Ventral Attention Systems: Distinct Neural Circuits but Collaborative Roles. *The Neuroscientist*, *20*(2), 150–159. https://doi.org/10.1177/1073858413494269

Wheelock, M. D., Culver, J. P., & Eggebrecht, A. T. (2019). High-density diffuse optical tomography for imaging human brain function. *Review of Scientific Instruments*, *90*(5), 051101. https://doi.org/10.1063/1.5086809

Wijeakumar, S., Huppert, T. J., Magnotta, V. A., Buss, A. T., & Spencer, J. P. (2017). Validating an image-based fNIRS approach with fMRI and a working memory task. *NeuroImage*, *147*, 204–218. https://doi.org/10.1016/j.neuroimage.2016.12.007

Xu, Z., Adam, K. C. S., Fang, X., & Vogel, E. K. (2018). The reliability and stability of visual working memory capacity. *Behavior Research Methods*, *50*(2), 576–588. https://doi.org/10.3758/s13428-017-0886-6

Yebra, M., Galarza-Vallejo, A., Soto-Leon, V., Gonzalez-Rosa, J. J., de Berker, A. O., Bestmann, S., Oliviero, A., Kroes, M. C. W., & Strange, B. A. (2019). Action boosts episodic memory encoding in humans via engagement of a noradrenergic system. *Nature Communications*, *10*(1), 3534. https://doi.org/10.1038/s41467-019-11358-8

Vita

Kaleb T. Kinder was born in Cape Girardeau, Missouri in 1992 and grew up in the Midwest. He graduated from Goreville High School in 2011 and earned his bachelor's degree, cum laude, in Psychology in 2015 from Southern Illinois University, Carbondale. At Southern Illinois University, Carbondale, he worked as a research assistant in the Integrative Neuroscience Lab and Contextual Behavioral Science Lab. In 2015, he worked as a research assistant at the University of Geneva, Switzerland in the Laboratory of Neurology and Imaging of Cognition. In the fall of 2016, he joined the Attention, Brain, and Cognition Lab at the University of Tennessee, Knoxville, to pursue his Ph.D. under the mentorship of Aaron Buss. At the University of Tennessee, Knoxville, his research focused on how executive functions support goal-directed behavior. His approach involved using a combination of neuroimaging and continuous behavioral measures to investigate selective attention and memory, and how they interact with the motor system. He is expected to graduate in May 2023 with a Doctor of Philosophy degree in the Cognitive and Developmental Science program.